МІНІСТЕРСТВО ОСВІТИ І НАУКИ УКРАЇНИ
НАЦІОНАЛЬНИЙ АВІАЦІЙНИЙ УНІВЕРСИТЕТ
НАЧАЛЬНО-НАУКОВИЙ АЕРОКОСМІЧНИЙ ІНСТИТУТ
КАФЕДРА ЗБЕРЕЖЕННЯ ЛЬОТНОЇ ПРИДАТНОСТІ АВІАЦІЙНОЇ ТЕХНІКИ

ДОПУСТИТИ ДО ЗАХИСТУ
Завідувач кафедри
д-р техн. наук, проф.
_____ О.В. Попов
«__»_____2021 р.

ДИПЛОМНА РОБОТА (ПОЯСНЮВАЛЬНА ЗАПИСКА)

ВИПУСКНИКА ОСВІТНЬОГО СТУПЕНЯ МАГІСТРА

ЗА ОСВІТНЬО-ПРОФЕСІЙНОЮ ПРОГРАМОЮ
«ТЕХНІЧНЕ ОБСЛУГОВУВАННЯ ТА РЕМОНТ ПОВІТРЯНИХ СУДЕН І АВІАДВИГУНІВ»

Тема: «метод оцінки впливу режиму роботи та технічного стану високотемпературного ГТД на процес накопичення пошкоджень в робочих лопатках турбіни»

Виконав: **_____ Р. Р. Нагірний**

Керівник: д-р техн. наук, проф. **_____ О. С. Якушенко**

Консультанти з окремих розділів пояснювальної записки:

охорона праці: канд. техн. наук, доц. **_____ В. В. Коваленко**

охорона навколишнього середовища:
канд. техн. наук, доц. **_____ Т. В. Саєнко**

Нормоконтролер **_____**

Київ 2021

NATIONAL AVIATION UNIVERSITY

Institute: *The Aerospace Faculty*
Faculty: *The Aircraft Faculty*
Department: *Aeroengines Department*
Educational and Qualifications degree: *Master*
The specialty: 272 Maintenance and Repair of Aircraft and Aeroengines

APPROVED BY

Head of the Department

_____ Y. M. Tereshchenko

"____"_____2021

Graduation Diploma Work Assignment

Student's name: NAHIRNYI RUSLAN ROMANOVICH

1. The Work (Thesis) topic: *Method for assessing influence of operating mode and technical state of high-temperature gas turbine engine on the process of damage accumulation in its turbine blades.*

Approved by the Rector's order of 04 "October", 2021 № 2137/ст.

2. The Graduation Project to be performed: *October 25-2021—December 22-2021.*

3. Initial data for the project: *TFE should be designed for standard atmospheric conditions: T amb=288 K, P amb = 101.3 kPa, Tg_t=1550K.*
4. The contents of the explanatory note (the list of problems to be considered):.

5. The list of mandatory graphic materials:

6. Schedule of Graduation Work Performing

Stages of Graduation Work Completion	Stages Completion Dates	Remarks
Literature review of materials concerning the project	28.09.21-15.10. 21	
Modeling thermo and gas dynamic parameters of TFE engine	15.10.21-07.11.21	
Modeling multi-mode model of TFE workflow	08.11.21-20.11.19	
Modeling damage accumulation model	21.11.21-30.11.21	
Labor precaution	01.12.21-12.12.21	
Environmental protection	01.12.21-12.12.21	
Arrangement of graphical part of diploma work	12.12.21-18.12.21	
Preparation of explanatory note	14.12.21-20.12.21	

7. Advisers on individual sections of the work (Thesis):

Section	Adviser	Date, Signature	
		Assignment Delivered	Assignment Accepted
Labor precaution	Kovalenko V. V.		
Environmental protection	Sayenko T. V.		

8. Assignment issue date _____

Graduate Project Supervisor *O. S. YAKUSHENKO*
(supervisor signature)

Assignment is accepted for performing:
Graduate student *R. R. NAHIRNYI*
(graduate student's signature) (Date)

CONTENT

INTRODUCTION

Gas turbine engines are the main type of engines in civil and military aviation, used in shipbuilding, energy, gas industry. The most important requirement for engines, especially aircraft engines, is high reliability.

In the problem of ensuring the reliability of gas turbine engines, an important role belongs to the reliability of the most common parts - blades. The blades are complex, highly loaded critical parts that experience a complex complex of influences of various nature (static loads, vibrations, heating) for a long time of operation. Blade breakage leads to serious accidents, material losses.

Therefore, to ensure the reliability of the GTE, it is necessary to know when these blades fail before they cause a catastrophe, so various bench tests are performed during the design to assess the life of the blades, but bench tests are usually expensive and must be based. For this, mathematical models are being developed during the design to help assess durability, but the engine is not operating in ideal conditions.

The most significant impact on the durability of elements and components of aviation gas turbine engines have external environmental conditions, as well as the conditions of flight operation. Therefore, it is very important to be able to estimate the accumulation of damage so that the residual resource can be understood.

Chapter 1 Methods for determining resource indicators of GTE and damage models

1.1 Durability and factors that affect it

Durability is the property of the object to perform the necessary functions before the transition to the limit state with the installed system of maintenance and repair [1]. When the limit state - a state in which further use of equipment, as intended, is unacceptable. The processes of wear, aging, various loads, such as temperature or centrifugal, which develop during the operation of equipment at specified modes, as well as timely maintenance, all these factors affect the durability of blood pressure. . However, it does not take into account the destruction or failure of the element due to manufacturing defects (which may be cracks, scratches, dents) or due to accidental causes.

All these factors that affect durability can be divided into 3 groups, namely:

Strength factors include design, production, technological, load and temperature factors. They occur due to the concentration of stresses in structural elements and residual stresses arising from imperfect technology and due to plastic deformations during assembly or repair, and depend on the properties of materials and their changes during operation. The external environment, classified according to the effect on the structure of simultaneously and separately acting factors that determine the load, exerts the decisive influence on the aircraft structure. Dynamic loads differing in amplitude-frequency characteristics, stress gradient, average voltage of exposure duration, etc. [2], exert a special influence.

Operational factors include: flight modes differing in speed, altitude, used maneuvers, aircraft flight weight; runway condition; the duration of taxiing and towing on the runway; individual characteristics of crew members and their professional training; meteorological and climatic conditions of flights, including atmospheric turbulence, temperature gradients along the height, snow, hail, etc .; the qualifications of the technical-engineer personnel(TEP), determined, in particular, by knowledge of the aircraft design, the completeness of detecting malfunctions and damages, the places of initial crack

development, the timeliness and effectiveness of measures to localize and eliminate them; the quality and completeness of preventive measures, as well as the quality of use of the used means of monitoring the technical condition of aircraft, etc. [2].

Organizational factors include: technical general engineering and special TEP training; selection of appropriate strategies and methods; complexity in carrying out maintenance forms according to the adopted program and carrying out current repairs; timeliness in providing production with spare parts in the event of failures and performing current repairs; applied methods and means of mechanization and automation of aircraft preparation processes for flights; search for malfunctions, failures and their elimination; performance of other work related to the preparation of aircraft for flights, in particular the use of automated means of monitoring the technical condition of all functional systems of the aircraft, etc. [2].

The design and creation of modern aircraft consumes a large number of resources, as well as the production of new, more cost-effective aircraft, makes it necessary to determine and ensure the appropriate durability, as well as the appropriate duration of use of the aircraft for its intended purpose. This creates problems with different durabilities, such as:

Physical durability - the same durability as described above, its basis is the properties of the structure, its components, namely the material to have endurance to withstand operating loads. If simpler, it is determined by the resistance of the material or structure to fatigue, corrosion (damage from it) and wear of individual components (for the structure).

Economic durability - durability that depends on the profitability of the use of a particular aircraft. When the price of maintenance exceeds the profit from the use of aircraft, we can safely say that the economic durability of this technique has come to an end.

Moral durability - longevity that depends on the development of aviation. Our world, and especially scientific and technological progress, is not standing still, new composite materials are being created that make the aircraft lighter, and it can fly at a lower weight but with the same characteristics. We should also not forget about advanced production

technologies or methods of calculating long-term strength, and the use of the concept of "permissible damage" always makes it possible to reduce the weight of structures and meet the requirements. In turn, the development of engine-building improves and creates more economical options for turbojet engines with lower fuel consumption. All this is the cause of aging technology, construction and its components, so it is replaced by newer and more perfect. This type of longevity is incalculable and is only a sociological concept. But when designing a designer must take into account all the durability.

1.2 Life cycle of machine

Durability can be quantified as a operational life or service life. We consider the operational life of the object from the beginning (or restoration) to the transition to the limit state, when the service life is the same resource, but in calendar form.

Operational life is determined at 2 stages of the life of the structure, namely its design and operation.

We consider the design resource to be the time interval that was determined during the design or certification of the structure or its element, during the design resource provides the required level of structural safety in terms of strength.

During design the possibilities of a design to maintain loadings which are necessary for a resource which is established by requirements are forecasted and also provided..

During operation, it is important to predict the residual life, under certain conditions of structural damage.

In the world, there are concepts of providing a resource at a safe level that allows the operation of equipment or its structures at the calculated loads. These concepts ensure the safety of the structure under strength conditions (SSC)

The designer in the design of equipment, construction or its element can use one of the principles that will meet the requirements of SSC:

1. Safe life
2. Fail-safe

3. Permissible damage

Safe-life(or safe resource) of a structure is that number of parameters such as flights, landings, or flight hours, during which there is a low probability that the strength will degrade below its design ultimate value due to fatigue cracking[5]

This concept is very common and has been used for decades, its use began in the 50s of last century, it was then that civil aviation began to develop rapidly.

To ensure flight safety and prevent fatigue failure of aircraft structures in operation, their service life is significantly limited, followed by a gradual extension to the operating area, where the occurrence of fatigue damage is unlikely (Fig. 1.1a). This does not require careful monitoring of operational damage. [3]

It is obvious that most of the park has a high fatigue life, and the resource of these structures is not fully used: it is a fee for security [3].

The concept of safe resource accepts the fact that there is an accumulation of damage, but the strength properties of the structure must be higher than the level that is allowed to operate, so there is no need to assign additional or special maintenance

The structure is operated for a limited time, measured in hours or number of load cycles, and further operation beyond these limits is assumed that the accumulated damage can lead to the destruction of structural elements. At the same time, the principle of step-by-step establishment and extension of assigned resources (up to decommissioning of aircraft) according to the conditions of durability during long-term operation is applied [3].

Specified life time - the total operating time of the object, at which the operation must be stopped regardless of its state [4].

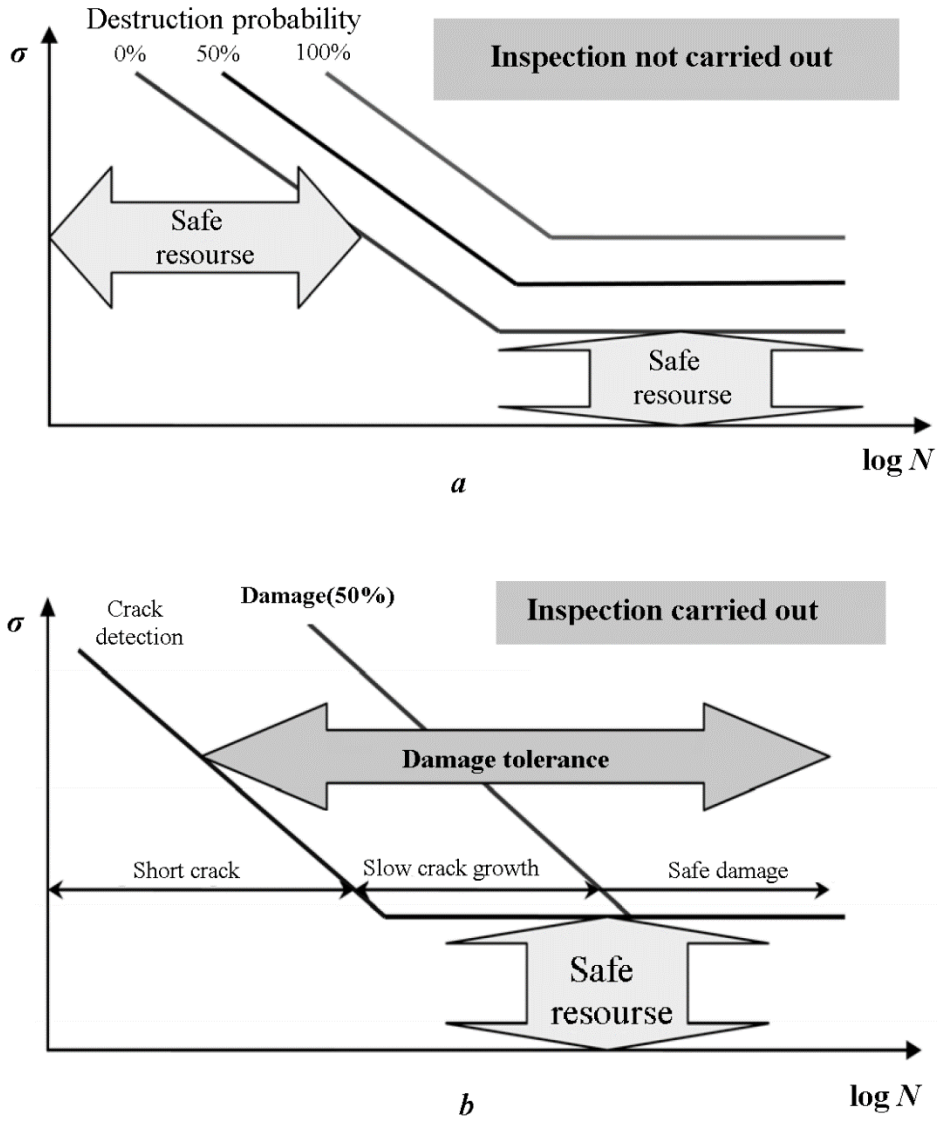

Fig. 1.1 Scheme of presentation of the basic concepts of design of aircraft structures on the example of fatigue curves: the concept of safe resource (a); concepts of damage tolerance and safe damage (b).

The specified life is divided into:

- advance assigned operating time;
- primary assigned operating time;
- assigned operating time to fist repair;
- overhaul time;
- warranty operating time.

Advance assigned operating time – service life, which is established when the product is transferred for tests[3].

Primary assigned operating time – service life, installed before the start of operation of the first serial product [3].

Assigned operating time to fist repair – service life from start of operation to the first repair [3].

Overhaul operating time – operating time of an object or a resource between repairs that were in a row.

Warranty operating time – operating time of the object (in hours, cycles or other units), during which the manufacturer guarantees its trouble-free operation, provided that the consumer observes the operating rules, including the rules for storage and transportation [4]

Fail-safe is the attribute of the structure that permits it to retain its required residual strength for a period of unrepaired use after the failure or partial failure of a principal structural element [5]

To ensure fail-safe, the following are used: materials that are well resistant to fatigue, namely the growth of cracks, during loads (cyclic); structures in which the load is distributed in parallel ways; structures that will stop the spread of cracks.

Tolerance of damages. This concept generally follows the concept of tolerable damage, but with one but, namely, the emphasis on the fact that defects may be in the design at an early stage of operation. The basic principles of this concept are the provisions of "slow growth of cracks" and also the principle of safe damage.

The concept of damage tolerance covers a large number of concepts and principles, here is one of its definitions: «Damage tolerance is the attribute of the structure that permits it to retain its required residual strength for a period of use after the structure has sustained a given level of fatigue, corrosion, accidental or discrete source damage[5]».

1.3 Methods of operating time calculation

The operating time of the structure must meet the requirements of flight safety, and we should not forget about the economic side of the resource, namely the rational use of the structure, when the market, after a certain period of time will be more efficient and profitable structures.

All methods for calculating the operating time of structures are divided into:

Empirical methods. From the word empiricism it is clear that these methods use the experience already gained in the use or operation of structures. Therefore, the resource is defined as minimal, taking into account the existing identical designs, of course, the resource will be specified in the future. Aircraft leaders, they are the helpers in developing recommendations to clarify the resource, because they are the flying test samples that can be studied. Such leaders are specially equipped for experimental flights and help gather all the necessary information. This information helps to learn about weak structural elements before they appear on serial samples.

Leader aircraft provide the necessary time reserve for engineers who are developing documentation to prevent the development of education and the development of defects on the serial sample, as the leaders fly with the park. Although their number is less than the serial samples. Therefore, they use forced operating programs to prevent the formation of damage on serial models.

Leading efficiency will be achieved when the accumulation of fatigue damage on the leader occurs 3-5 times faster than on the park facilities [4]

The disadvantages of this method are the difficulty of determining the actual durability, as it is impossible to prevent damage that could lead to disaster, due to this possible underestimation of durability and in the future is not rational use of the structure. The disadvantages include the possibility of damage to the structure, due to incorrectly calculated resource, as there is no guarantee that the durability was determined correctly.

Calculation methods. The basis of these methods is the assumption of limiting the durability of the properties of the structure, to resist fatigue.

The hypothesis of a linear rule of summation of damages has become the most common. This hypothesis states that the linear function of load cycles describes fatigue failure, and has the form:

$$\sum_{i=1}^{k} \frac{n_{c_1}}{N_c} = 1$$

where $\frac{n_{c_1}}{N_c}$ - relative damage to the structure

n_{c_1} – load cycles

N_c – the total number of cycles before destruction

k – number of load blocks

But this hypothesis has disadvantages, namely, studies show that it gives false durability, in some cases greater, in some cases less than real. It is clear that it is very dangerous to have inflated longevity, as it can lead to disaster. This reason for overestimation is a consequence of not taking into account all the influencing factors. Therefore, in order for the formula to take these factors into account, it needs to be modified:

$$\sum_{i=1}^{k} \frac{n_{c_1}}{N_c} = m$$

where m – a parameter that is determined experimentally

Of course, the introduction of m violates the idea of linear summation, as different from unity, but studies show that m has a large range, so the use of linear summation can be difficult

Experimental methods. These methods are based on experiments, namely testing of structural elements on stands. Such elements are tested at the same loadings, also loadings are chosen conditionally for this or that element of a design..

When withstanding conditional loads a given number of cycles, the element is considered satisfactory for use.

The disadvantages of these methods - the load on the stands do not correspond to the actual load during operation, which can lead to incorrectly determined durability, so it is used to compare samples.

1.4 Establishing and increasing the resource

Right installation of the resource is very necessary for flight safety and rational use of equipment, construction or its element. Therefore, to begin with, the resource should be limited to the workload of the most exposed elements, namely the blades and the turbine disk. It is the durability of these elements that forms the basis of the initial resource. Therefore, the calculation of durability should be carried out taking into account the most available factors, even the manufacturing technique can affect the durability of the blade.

This is followed by the experimental part, which helps to clarify the previously set resource limitations by theoretical calculations of the turbine blades and disks. Cyclic tests are usually performed. But since it can take quite a long time, due to their great durability, conduct accelerated testing. They are tested in special chambers to simulate their working conditions.

The information obtained after the tests is very important, as it serves as a basis for the assigned operational life, which in turn shows the work to the limit state.

The repair life of its installation and increase directly depends on the assigned resource, as occur within its boundaries. The same situation with the operation of the state. The assigned resource is also limited by the requirements set by flight safety.

At the first time of operation of the engine, its resource still remains imperfect, even with those calculations taking into account many factors and based on them bench tests, they can not show the resource in real operation. Therefore, at first, the engine is set to a

fixed resource with subsequent monitoring of the engine. Fixed resource is a resource that is installed in the early stages of operation, when the time spent in operation is not great, respectively, and reliability, such a resource is established by the method of a weak element. Installation by the method of a weak element means that it is determined by the element with the least durability, and as we know in the GTE it is the blades and blades of the turbine.

Bench tests are followed by full-scale flight tests in order to understand and bring the specified resource closer to the real one, as mentioned earlier, bench tests cannot fully convey the full-scale operating conditions of the GTE. Aircraft engines, for example, have in flight different from the bench range of speeds and pressures in front of compressors, other operating conditions of the system of prompting at low ambient pressure [7].

When long-term field tests are successful, you can finally establish the initial life of the engine. It is also possible to run ahead, this is when the engine starts running before the field tests are over.

Further increases in resource after production of the initial resource are based on operational experience. In order to increase the resource, the reliability of the first (leaders or "main") engines is satisfactory after the initial set resource τ, and their output exceeds the service life by $\Delta\tau$ hours, you can increase the resource and set it as $\tau 1 = \tau + \Delta\tau$

This is followed by operation on condition, but provided that the operation was successful and the engines have proven their high durability. To move to operational status, it should also be noted that the engine must have a system for diagnosing and monitoring engine parameters, and must also organize the collection and processing of information on engine diagnostics. The process of increasing the resource of an engine of a certain type is always a process of processing various multifaceted information and making a basic decision on this, that is, it is essentially a control process [7]. But with high of operational life, the process becomes much more complicated, due to the large number of necessary solutions to increase the resource for different elements for each engine. And operational operation requires the organization and management of a system that includes subsystems of different levels, interconnected and coordinated.

1.5 Models of fatigue

Fatigue fractures of metals are the result of alternating or repeated loads, and such fractures in this case require a significantly lower maximum load than static fracture.

Fatigue is a process of gradual accumulation of material damage under the influence of alternating stresses, leading to a change in its properties, the formation and development of cracks and destruction [9]

There are two main types of fatigue damage:

High-cycle fatigue is fatigue that occurs when stresses do not outweigh the elastic limit of the material. The process of high-cycle fatigue occurs as follows, namely, the material accumulates scattered damage in the grains of the material, in its weakest or most stressed places, when there are a lot of them and they are nearby, the grains form the nucleus of a fatigue crack, which is a stress concentrator and begins to grow at the following loads

To assess the resistance of a material to high-cycle fatigue failure, fatigue curves are plotted, usually their curves are plotted in the coordinates σ - N at a given cycle factor R. The number of cycles N is expressed in a logarithmic or natural scale (Fig. 1.2).

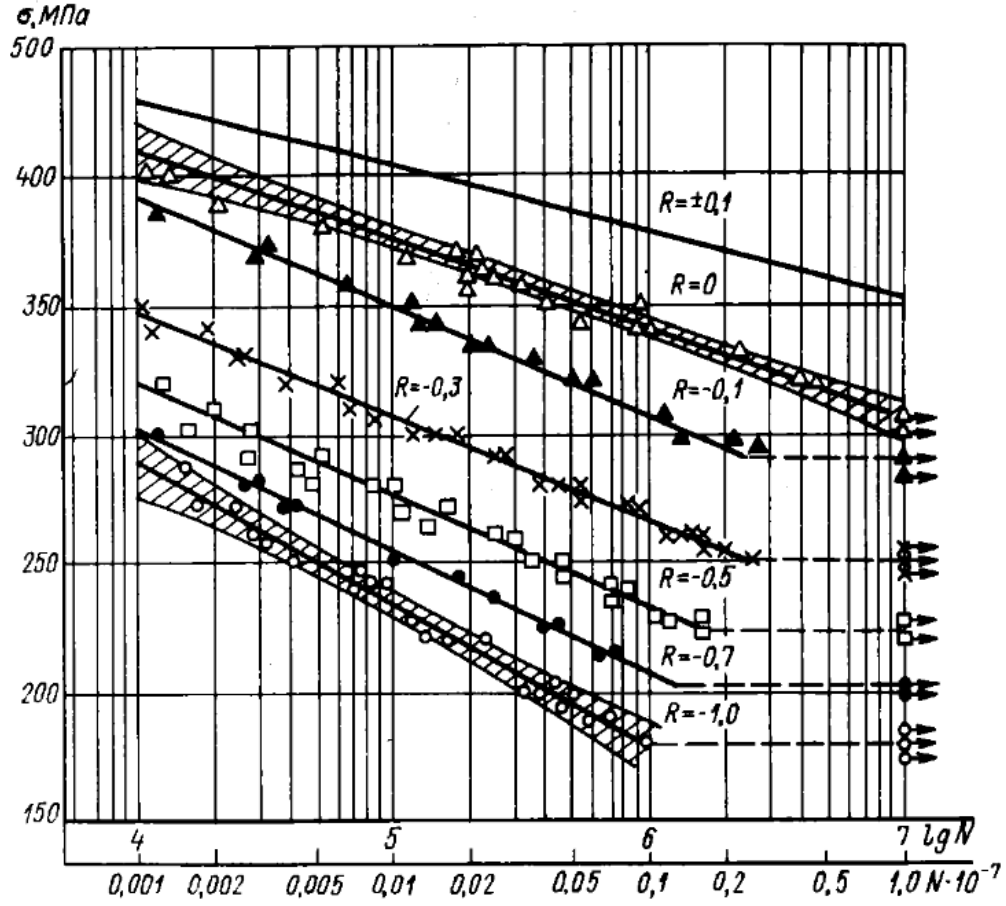

Fig. 1.2 High-cycle fatigue curves of 45 steel at different asymmetry coefficients of the tension-compression cycle

As mentioned above, the initiation of fatigue cracks occurs near stress concentrators, including microconcentrators (defects, micropores), therefore fatigue tests show a significant statistical spread.

Low-cycle fatigue is material fatigue in which fatigue damage or fracture occurs during elastoplastic deformation [11].

The boundaries between low-cycle fatigue, transition zone and high-cycle fatigue are arbitrary and depend on the plasticity of the material. Sometimes all fracture processes associated with cyclic inelastic deformation are referred to as low-cycle ones, i.e. anything that is not high-cycle fatigue. This approach is convenient, in particular, for low-plastic materials, in which the region is weakly expressed where elastic deformations can be neglected.

The fracture criteria for high-cycle fatigue can be written in both stresses and deformations, since they are uniquely related by Hooke's law. It is more convenient to write low-cycle fracture criteria using the values of plastic deformations rather than stresses. In the transition region (between high-cycle and low-cycle fatigue), when it is necessary to take into account the effect of both elastic and inelastic deformations, force, deformation, and energy criteria are used.

One of the simple criteria for low-cycle fatigue deformation is the Coffin criterion

$$N^{\alpha}\Delta\varepsilon = C$$

Where N is the cyclic durability, Δε is the plastic deformation range, α and C are empirical constants. Constant C is usually expressed in terms of the true ultimate strain in standard tensile tests.

1.6 Models of damage accumulated.

The development of the service life of machines and structures is mainly associated with the accumulation of irreversible damage in their parts, assemblies and elements. These damages are both mechanical (fatigue, wear, cracking, accumulation of plastic deformations) and physicochemical origin (corrosion, erosion, adsorption). Many types of damage are mixed. So, the processes of wear of rubbing parts can include phenomena of mechanical, physical and chemical origin.

Semi-empirical damage model.

The variety of the listed phenomena, they can be described within the framework of a unified semi-empirical theory linking the rate of damage accumulation with the existing loads and environmental conditions. none of the models of this theory aims to explain or describe in detail the phenomena. Semi-empirical models are used to solve engineering problems associated with calculating the durability and predicting the resource. The only purpose of these models is to provide calculation tools that are as simple as possible and use the minimum amount of experimental data as initial information.

Linear damage summation. The simplest and the most efficient method of developing the accumulation of effects in different modes of cyclic load. We take the

number of cycles to run up N, with the changeover σ, the total runnability is equal for the number of cycles n, if the function n / N is sufficient. Apparently, the additional information provided by the device, or the additional requirements, will be the mother of such a viewer n1 / N1 + n2 / N2 +… = 1.0.

The linear law of addition of damages has a number of shortcomings due to the fact that this law does not take into account in what sequence there were cyclic loadings. To that, great stress on the cob of exploitation, can lead to the adoption of serious jobs. If the material will be gradually loaded with higher loads, then this amount will be more than one, if on the contrary, the amount will be less than one

The phenomena of damage and destruction reveal a clear probabilistic nature, starting from the atomic-molecular level and ending with the level of a machine, structure or structure, therefore, the results of tests for durability have a significant statistical dispersion. Thus, the cyclic fatigue test life can change at the same stress amplitude by an order of magnitude or even more. Factors affecting the variation in mechanical properties include various defects (for example, cracks, inclusions and voids), as well as imperfections or instabilities in the process and quality control. The mechanical properties of structural metallic materials are not the same for different heats, and even more so for the products of different plants and suppliers, therefore, when predicting the resource at the design stage, it is necessary to take into account this component of the scatter of mechanical properties.

Structural Damage Model.

Semi-empirical models of damage accumulation do not include an explicit description of the physical phenomena that occur in the material during its damage. The scope of these models is limited by conditions that are more or less close to the conditions of basic life tests. Because of this limitation, difficulties arise when predicting the resource for a time significantly exceeding the test base, when transferring the test results of samples to large-sized products, as well as when assessing the probabilities of rare events. The listed difficulties to a certain extent disappear if, instead of semi-empirical models, we use models of damage accumulation and destruction based on structural considerations.

The structure of materials is very diverse, and the size of the material can be measured in the range of almost atoms and molecules to the size of the material, but it is not worth it to go deeper. Figure 1.3 shows a schematic scale of the various structures. It starts with a crystal lattice of *1* material and has dimensions of the order of 10^{-10} ... 10^{-9} m. Next comes the *2* molecular structure. The scale of *3* linear defect or crystal lattice violation is in the range from 10^{-9} to 10^{-7}m. When the distance between them is *4* from 10^{-8} to 10^{-4} m.

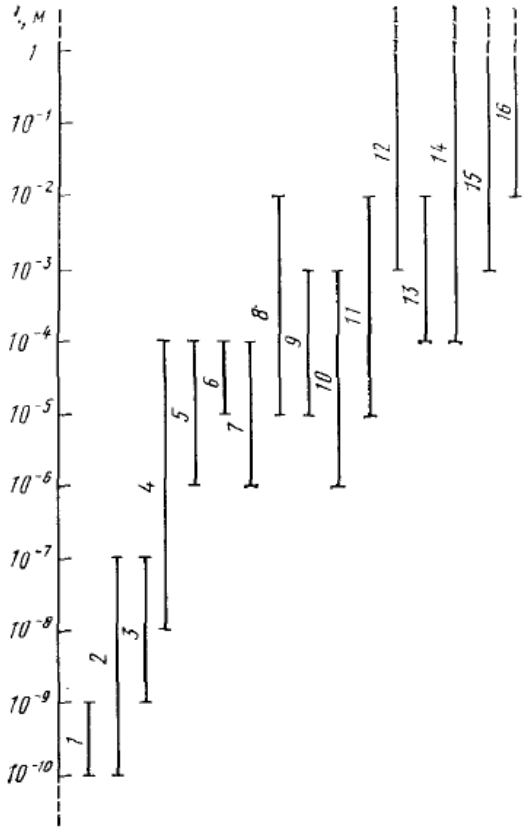

Fig. 1.3 Schematic characteristic scales of the structure

All of the above is what is considered by solid state physics. Then there are the elements that can be analyzed in both solid state physics and materials science. *5* and *6* are sliding lines and bands, respectively, *7* - micropores and microinclusions, *8* - grains and fibers, *9* - microcracks. *10* - micro-rough height, *11* - relief length, these are the properties of the material surface. Next comes the elements of material mechanics. *12* - macroscopic cracks, *13* - end plastic zones of these cracks, *14* - macroscopic technological defects, *15* - stress concentrators, *16* - the scale of changes in nominal stresses.

The process of damage accumulation, as well as destruction, includes all these elements, but the development of models that take into account all these elements would be extremely difficult, which is already unrealistic. Therefore, the models are built according to the following principle: a reference point is taken, namely one of the levels of the structure, we set the properties of the level as a basis, and at this level the way of interaction of structure elements is used, and with the help of this model, the behavior of the level above is predicted. Thus, we go, for example, from the scale level between dislocations to the level of microcracks, then from the level of microcracks to stress concentrators, etc. For real tasks, it is important to reach the level of the product as a whole. In order to stay within the framework of the application of continuum mechanics, it is enough to take structural elements with a size of about 10^{-6}m as the initial level [6]. Structural models are very important for composites. They are also important for combining the processes of damage and false destruction.

The main drawback of structural models is that a larger amount of information is needed than semi-empirical ones, and this information is difficult to obtain even from direct experiments, since the scales are very small.

Chapter 2 Mathematical model of project engine

2.1 Mathematical modelling

Today, mathematical modeling is an important part of design. It is difficult to imagine the development of a GTE without a mathematical model of it as a whole or certain nodes. So what is mathematical modeling?

Mathematical modeling is the process of creating an abstract model and operating with it in order to obtain information about a real object [12]. Under the mathematical model is understood a set of calculation formulas, computational algorithms, tabular, graphical results. Mathematical models are an information analogue of the product and solve the problems of analysis [12].

In most technical objects, mathematical modeling is divided into levels, such as macro-, micro-, and meta-levels, the difference between them in the details of the processes taking place in the objects.

The mathematical model at the micro level is a system of differential equations with partial derivatives that describe the processes of the environment with certain constraints set by the developers. The system of equations is of course known, but their solution is known only for specific cases. Therefore, the first thing to model is to build a primary approximate model.

The mathematical model at the macro level is a system of differential equations with already given initial conditions. The initial data can be component and topological equations that describe the relationship between the elements of the system.

Mathematical model at the metalevel level is a system with the most detailed processes, it allows in one mathematical model to show the relationship of all parts of the engine blocks.

Mathematical model is used to solve a large number of problems:

- performing a design calculation of the engine, as a result of which the main thermogasdynamic parameters of the engine, the geometric parameters of its flow path and other data are determined in accordance with the requirements of the technical task;
- to optimize the parameters of his workflow;
- calculation of high-altitude-speed, throttle and other operational characteristics of the engine with the known geometry of its flow path;
- for calculating transient, transient modes and many others.

At present, in the theory of aircraft engines for steady-state conditions, in most cases, mathematical models are used, which are based on a set of nonlinear algebraic equations.

Basic requirements for GTE models:

- accuracy to the real object - reflects the degree of similarity of calculations and real results;
- cost-effectiveness - time spent on calculation
- versatility - the ability to use for other similar engines without much effort to redesign the model
- modular structure to be able to replace, remove or add a module, or also if you need to improve the module
- correct construction of the hierarchy of the mathematical model
- simplicity of the model - the use of simple mathematical methods

Usually, the classification of mathematical models is based on the level of detail of the processes that occur in the engine, ie the elaboration of the connections between the input and output parameters. According to the level of sophistication and complexity of the models, they can be divided into 4 levels:

Zero level – GTE is represented as a "black box" (cybernetics). The model forms the connection of the main parameters of the engine with the input data of simple dependencies. The type of engine or its design does not affect the mathematical model.

The first level is a model where a zero level model is used for each engine unit (turbine, compressor, combustion chamber), and these levels are interconnected.. Relations

and equations are used that reflect the physical relationships between the units of the GTE with the assumptions typical for the engineering formulation of the problem.. Geometry at this level is not clearly shown, it is hidden in the characteristics of the nodes.

Second level - at this level the connections between the GTE units are already modeled in detail, ie the engine parts are modeled at the first level and their parts at the zero level. The geometry is already set and directly affects the engine parameters.

Third level – the description of compressor and turbine assemblies is presented at the level of blade rows; losses are calculated in detail using experimental and statistical data on their components. As a rule, a two-dimensional theory of the flow of the working fluid in the flow path of the engine is used, the geometric dimensions of the flow path are calculated, but all calculations are carried out for the average radius of the flow; the fourth level - the spatial gas flow in the engine flow path is modeled. These models are the most promising, but they are very complex.

Mathematical models make it possible to solve various problems related to a product or its unit, and in many cases replace expensive physical experiments..

2.2 Designed engine

For my projected engine, I took the CFM56-7 engine as a basis and, based on the prototype engine, developed a mathematical model for my parameters..

General understanding of the prototype engine

The prototype of my engine under development is compact and has a simple modular design. It has sufficient rigidity and has two housing parts that separate, this is the fan housing in front and the low pressure turbine in the rear of the engine (Figure 2.1). The input device used on this engine is unregulated, subsonic, and the reversing device is located in the outer loop. The low pressure compressor consists of a fan stage and three booster stages.

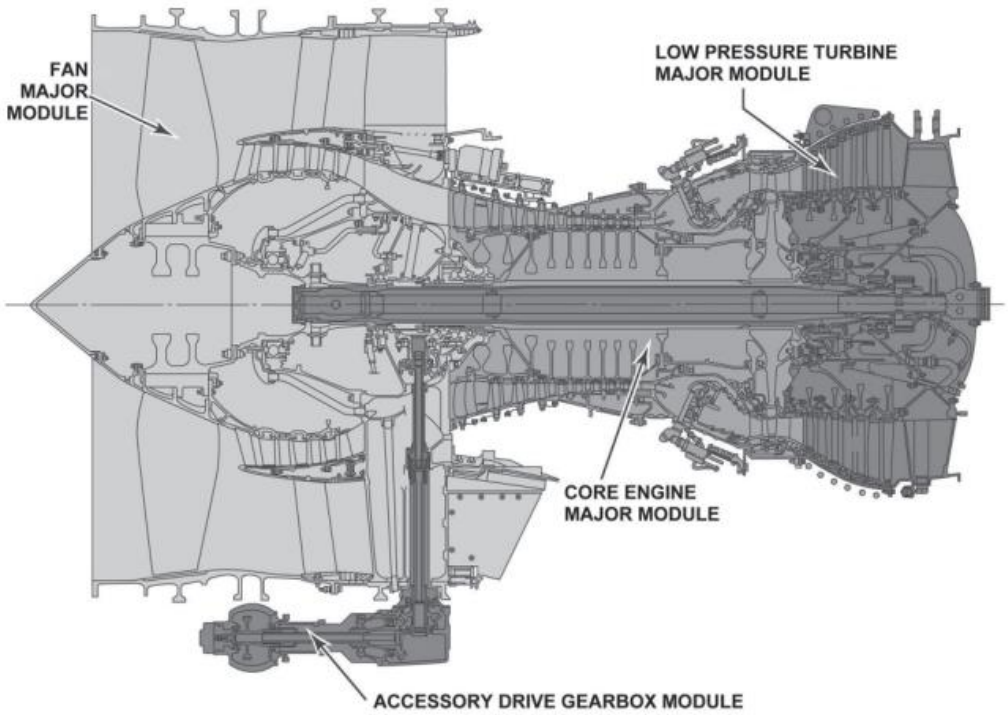

Fig. 2.1 Modular design

The prototype of my engine under development is twin-shaft, which means there are two rotating shafts: one is driven by a high-pressure turbine, the other is driven by a low-pressure turbine.

Fan module.

The prototype has a single-stage fan and also has a three-stage amplifier on the low pressure shaft The amplifier is called a low pressure compressor because it sits on the low pressure shaft and compresses the flow before it reaches the high pressure compressor..

The fan blades are made of titanium alloy and have shroud flanges in the middle part of the length. The fan blades have dovetail attachments for easy blade removal and replacement.

The fan casing is of a composite structure, it consists of a dividing casing, a retaining stage casing and a fan casing.

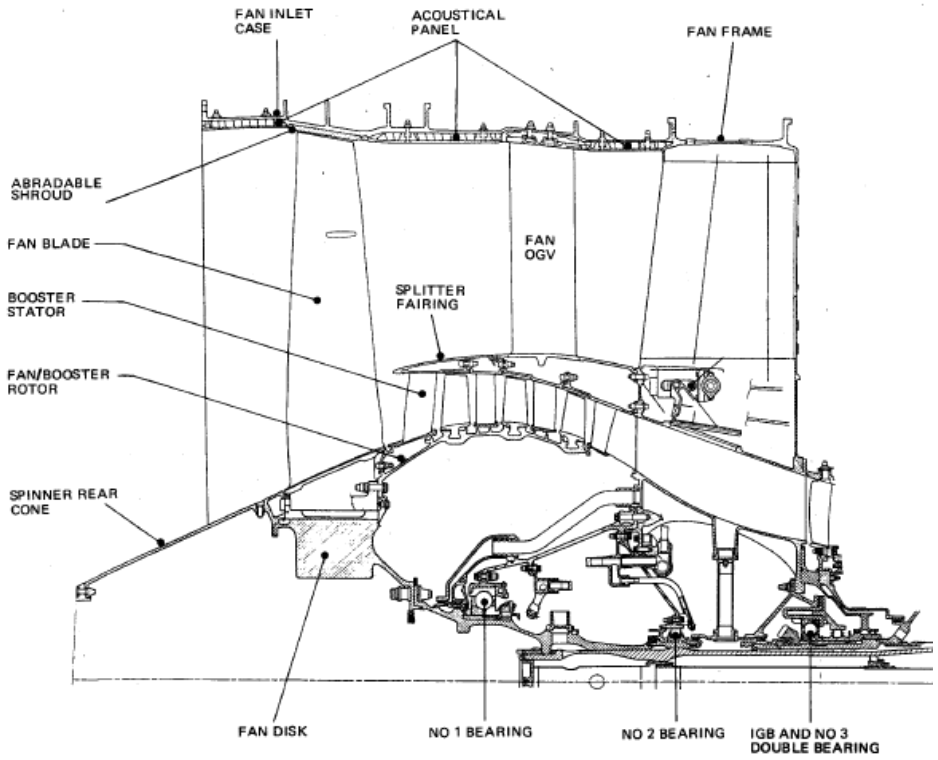

Fig 2.2 Major fan module

The blade crowns of the guide vanes are mounted in the casing of the retaining stages. The shroud blades of the guide vanes have a honeycomb covering, which contacts the combs of the labyrinth seals provided on the rotor drum of the low-pressure compressor

The rotor of the retaining stages includes a drum with rotor blades installed on it. The rotor drum, forged from titanium alloy, is attached to the rear of the fan disc. On the outer part of the drum, three annular grooves are milled for attaching the blades of the second, third and fourth stages.

Gas generator module

The gas generator has nine stages in the high-pressure compressor; to increase efficiency and gas-dynamic stability, the blades on the water have direction regulation (Fig. 2.3). The front casing of the HPC is attached to the flange of the fan casing with its front flange, and the rear flange to the front flange of the outer casing of the combustion chamber. In the rear part of the front compressor casing, in the area of the fifth and sixth compressor stages, there are technological windows for bleeding air into the active control system of radial clearances, for cooling the turbine and for the aircraft's own needs. The

rear compressor casing also consists of two parts that are split in the horizontal plane and accommodates the blades of the guide vane from the sixth to the ninth stage.

The HPC rotor consists of three parts:

- from the first to the second stage, the drum-disk part;
- disc of the third stage;
- from the fourth to the ninth stage disc drum part.

HPC blades from the first to the third stage are fixed individually on the drum-disk and disk parts of the rotor.

The annular combustion chamber is a continuous ring. It consists of an outer annular wall, an inner annular wall and forty combined frontal devices used for high-quality mixing of air with atomized fuel.

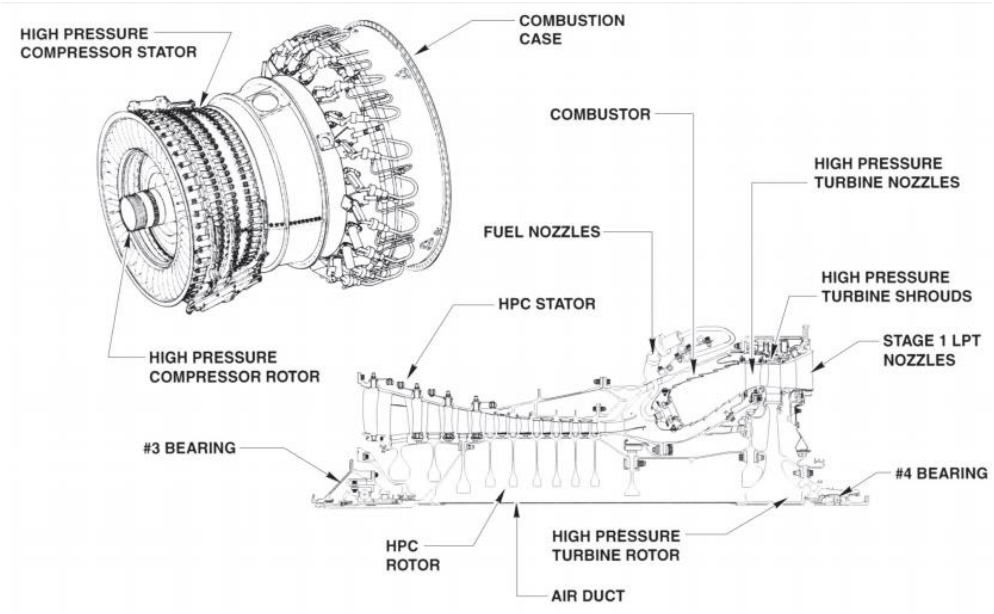

Fig 2.3 Core engine major module

High pressure turbine, single stage. It includes a crown of stationary stator blades of a nozzle apparatus of a block design (two blades in a block) and a crown of rotor blades installed on the disk in individual locking grooves of the "herringbone" type.

The blades of the nozzle apparatus and the working blades of the LPT are cooled, their profile and locking parts of the working blades are cooled by air due to the ninth stage of the compressor, passing through special holes into the inner and outer ends of the blades

and exiting through the perforated holes in the trailing and leading edges. A deflector is provided in the front part of the disk, which serves to control the flow of cooling air to the rotor blade, providing the required air pressure in the cavity between the deflector and the disk using a system of labyrinths above and below the spinner. The rear part of the disc develops into a cone, to the flange of which the LPT rotor journal is attached. Mixed air is supplied to the air cavity between the shroud shelves of the rotor blades / nozzle blade mountings and the combustion chamber housing, which is taken after the ninth and fifth stages of the HPC in order to ensure the operation of the system of active control of radial clearances. The same air is used to cool the blades of the nozzle apparatus of the first stage of the injection pump.

Low pressure turbine module

The low-pressure turbine is four-stage and consists of a stator and a rotor (Fig. 2.4). The stator part consists of a front and rear housing. The front housing of the injection pump contains the blades of the nozzle apparatus of the second, third and fourth stages and the stationary elements of the gas seal. On the outer surface of the front housing of the injection pump, a collector of the active control of radial clearances is mounted.

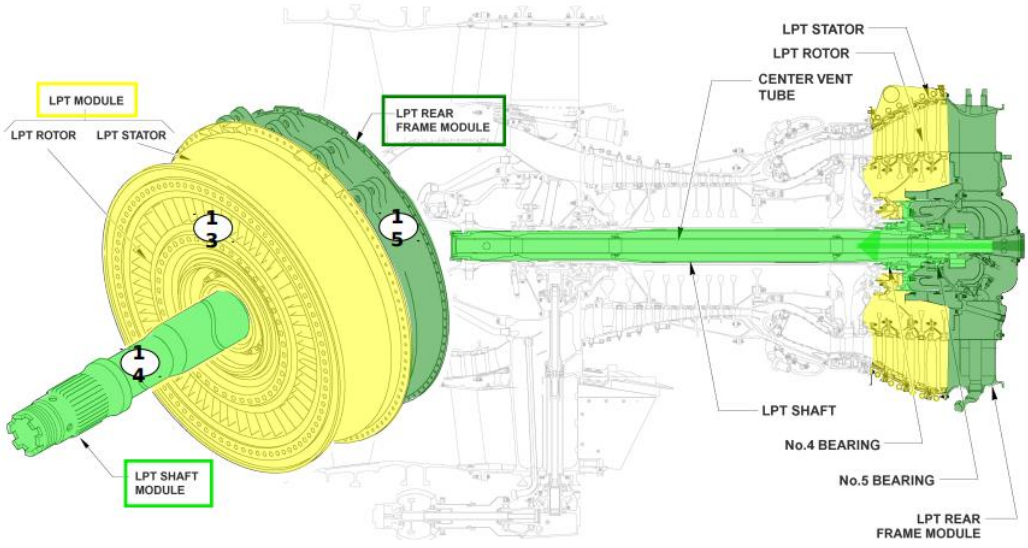

Fig. 2.4 Low Pressure Turbine major module

Process ports are provided in the lower part of the housing for visual inspection of the low-pressure turbine. On the second-stage nozzle blade, holes and casings are provided for mounting thermoelectric temperature sensors 6. The rear housing of the injection pump

is included in the power circuit of the engine and serves to accommodate the fifth support, to straighten the gas flow, to ensure that the engine is mounted in the rear plane; eye. Through two of the sixteen radial struts pass the oil supply and oil drainage pipes of the fifth support.

2.3 TFE thermodynamic and gas-dynamic calculations

For creating the linearized second level mathematical model of my design engine I using manual [13].

The initial data for calculation:

Altitude ..... $H = 0\ m$;

Velocity of flight $V = 0\ m/s$;

Thrust $P = 111000\ N$;

Total pressure ratio in the compressor $\pi_{\sum} = 32.7$;

Pressure ration in the fan $\pi_{fan}^{*} = 1.65$;

Bypass ratio $m = 5.3$;

Gas temperature before turbine $T_g^{*} = 1550\ K$;

Gas constant of air flow $R = 287.3\ \frac{J}{kg*K}$;

Gas constant of gas flow $R_g = 287.3\ \frac{J}{kg*K}$;

Adiabatic level for air $k = 1.4$;

Adiabatic level for gas $k_g = 1.33$;

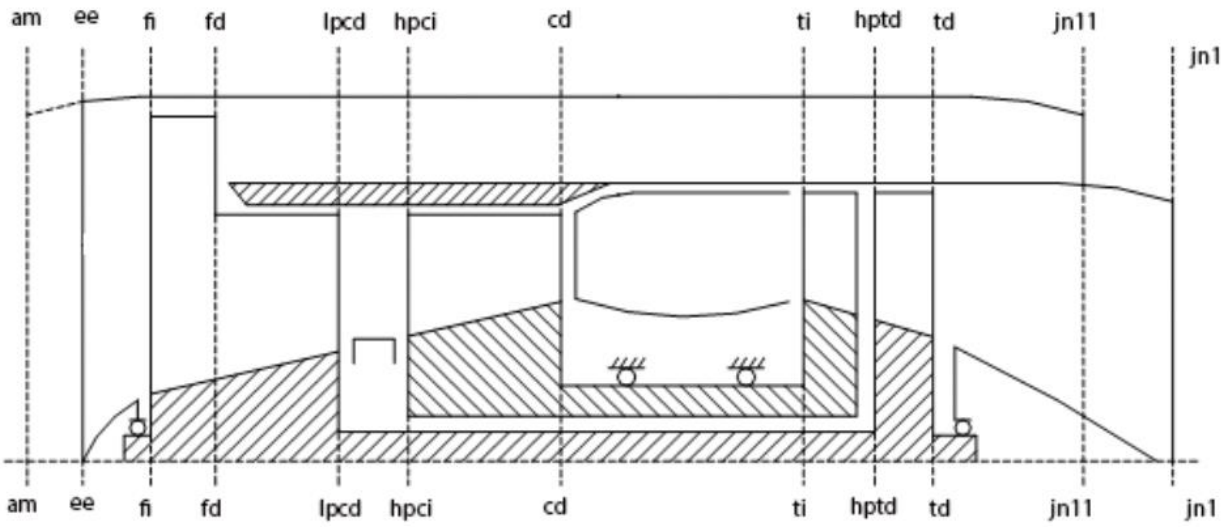

Fig. 2.5 Schematic figure of designed engine

1. The air parameters determination in an undisturbed flow in front of the engine (station am)

Let's find total pressure and total temperature for design flight altitude H=0

$$T^*_{am} := T_{am} + \frac{k-1}{k} \cdot \frac{V^2}{2R} = 288.15 + \frac{1.4-1}{1.4} \cdot \frac{0^2}{2 \cdot 287} = 288.1 = 288.1 \ K$$

$$p^*_{am} := p_{am} \cdot \left(\frac{T^*_{am}}{T_{am}} \right)^{\frac{k}{k-1}} = 101325 \cdot \left(\frac{288.1}{288.15} \right)^{\frac{1.4}{1.4-1}} = 101263.0 = 101263 \ Pa$$

2. The air paameters determination at the entry to the fan (station fi)

The total air temperature is

$$T^*_{fi} := T^*_{am} = 288.1 \ K$$

The total pressure recovery coefficient in the inlet $\sigma_i := 0.995$ and p*fi is determined by the formula

$$p^*_{fi} := p_{am} \cdot \sigma_i = 101325 \cdot 0.995 = 100818.0 = 100818 \ Pa$$

3. The air parameters determination behind the fan in the secondary flow (station fd)

The fan efficiency as η.fanI = 0.85

The work of air compression in the fan is calculated by the formula, J:

$$L_{fanII} := \frac{k}{k-1} \cdot R \cdot T^*_{fi} \cdot \left(\pi^*_f{}^{\frac{k-1}{k}} - 1 \right) \cdot \frac{1}{\eta_{fanI}} = \frac{1.4}{1.4-1} \cdot 287 \cdot 288.1 \cdot \left(1.65^{\frac{1.4-1}{1.4}} - 1 \right) \cdot \frac{1}{0.85} = 52370.0 = 52370$$

The total air temperature is:

$$T^*_{fdII} = T^*_{fi} + \frac{k-1}{k} \cdot \frac{L_{fanII}}{R} = 288.1 + \frac{1.4-1}{1.4} \cdot \frac{52370}{287} = 340.2 = 340.2 \ K$$

The total pressure is:

$$p^*_{fdII} := p^*_{fi} \cdot \pi^*_f = 100818 \cdot 1.65 = 166349.0 = 166349 \ Pa$$

4. The air parameters determination at the exit from the secondary flow jet nozzle (station jnII)

The total temperature is, K:

$$T^*_{jnII} := T^*_{fdII} = 340.2$$

Taking into account that the secondary flow of the engine has a short length, we accept total pressure recovery coefficient in the secondary flow as σ.sf=0.995. Then total air pressure before jet nozzle can be found by the formula:

$$p^*_{inII} := p^*_{fdII} \cdot \sigma_{sf} = 166349 \cdot 0.995 = 165517.0 = 165517 \ Pa$$

The jet nozzle pressure ratio:

$$\frac{p^*_{inII}}{p_{am}} = \frac{165517}{101325} = 1.634$$

The jet nozzle pressure ratio is less than the critical jet nozzle pressure ratio

$$\pi_{jncr} := \left(\frac{k+1}{2} \right)^{\frac{k}{k-1}} = 1.893$$

that's why the jet velocity of the fan air from the jet nozzle is determined by the formula for full expansion mode, accepting φ.jnII = 0.985

$$c_{jnII} := \varphi_{jnII} \cdot \sqrt{2 \cdot \frac{k}{k-1} \cdot R \cdot T^*_{jnII} \cdot \left[1 - \left(\frac{p_{am}}{p^*_{inII}}\right)^{\frac{k-1}{k}}\right]} = 0.985 \cdot \sqrt{2 \cdot \frac{1.4}{1.4-1} \cdot 287 \cdot 340.2 \cdot \left[1 - \left(\frac{101325}{165517}\right)^{\frac{1.4-1}{1.4}}\right]}$$

$$c_{jnII} = 294.5 \ \frac{m}{s}$$

5. The air parameters determination behind the compressor (station cd)

$$T^*_{jnIIst} := T^*_{jnII} - \frac{k-1}{k} \cdot \frac{c_{jnII}^2}{2 \cdot R} = 340.2 - \frac{1.4-1}{1.4} \cdot \frac{294.5^2}{2 \cdot 287} = 297.0 = 297\,K$$

Setting compressor stage efficiency η*.st = 0.91, we determine compressor efficiency by the approximate formula:

$$\eta^*_c := \frac{\pi^*_c^{\frac{k-1}{k}} - 1}{\pi^*_c^{\frac{k-1}{k \cdot \eta^*_{st}}} - 1} = \frac{31.2^{\frac{1.4-1}{1.4}} - 1}{31.2^{\frac{1.4-1}{1.4\,0.91}} - 1} = 0.8597 = 0.86$$

The work of air compression in the compressor is found by the equation, J:

$$L_c := \frac{k}{k-1} \cdot R \cdot T^*_{ci} \cdot \left(\pi^*_c^{\frac{k-1}{k}} - 1\right) \cdot \frac{1}{\eta^*_c} = \frac{1.4}{1.4-1} \cdot 287 \cdot 288.1 \cdot \left(31.2^{\frac{1.4-1}{1.4}} - 1\right) \cdot \frac{1}{0.8597} = 562971.0$$

The total air temperature behind the compressor is:

$$T^*_{cd} := T^*_{ci} + \frac{k-1}{k} \cdot \frac{L_c}{R} = 288.1 + \frac{1.4-1}{1.4} \cdot \frac{562971}{287} = 848.5 = 848.5\ K$$

The total air pressure behind the compressor is:

$$p^*_{cd} := p^*_{ci} \cdot \pi^*_c = 101263 \cdot 31.2 = 3.159e6 = 3159000\ \ Pa$$

6. The gas parameters determination behind the combustion chamber (station ti)

Setting total pressure recovery coefficient in the combustion chamber σ.cc=0.98, we find total air pressure before the turbine:

$$p^*_{ti} := p^*_{cd} \cdot \sigma_{cc} = 3159000 \cdot 0.98 = 3.096e6 = 3096000 \text{ Pa}$$

The turbine inlet temperature T^*_{ti} is given in the initial data:

$$T^*_{ti} := T^*_G = 1550 \text{ K}$$

The average specific heat of gas in the combustion chamber is found by the formula:

$$c_p := 878 + 0.208 \cdot \left(T^*_{ti} + 0.48 \cdot T^*_{cd}\right) = 878 + 0.208 \cdot (1550 + 0.48 \cdot 848.5)$$

$$c_p = 1285 \quad \frac{J}{kg \cdot K}$$

Setting combustion efficiency η.cc = 0.99 and accepting net calorific value of fuel H_u = 43000000 J/kg we determine relative fuel consumprion:

$$g_f := \frac{c_p \cdot \left(T^*_{ti} - T^*_{cd}\right)}{\eta_{cc} \cdot H_u} = \frac{1285.0 \cdot (1550 - 848.5)}{0.99 \cdot 43 \cdot 10^6} = 0.02118 = 0.021$$

Setting quantity of air, theoreyically required for complete combustion of one kg of fuel l_0 = 14.9 we find the average excess air/fuel ratio α in the combustion cahmber by the formula:

$$\alpha := \frac{1}{g_f \cdot l_0} = \frac{1}{0.02118 \cdot 14.9} = 3.169 = 3.169$$

7. The gas parameters determination behind the turine (station td)

Choosing relative quantity of compressor-bleed air for cooling the turbine parts g.cool=0.027 and accepting mechanical efficiency η.m=0.995we determined effective work of all stages of turbine from the following equation:

$$L_t := \frac{m \cdot L_{fanII} + L_c}{(1 + g_f) \cdot (1 - g_{cool}) \cdot \eta_m} = \frac{6 \cdot 52370 + 562971}{(1 + 0.02118) \cdot (1 - 0.027) \cdot 0.995} = 887270.0 \text{ J}$$

Accepting turbine efficiency η*.t = 0.9we calculate the turbine outlet temperature and turbine outlet pressure by the formulas:

$$T^*_{td} := T^*_{ti} - \frac{k_g - 1}{k_g} \cdot \frac{L_t}{R_g} = 1550 - \frac{1.33 - 1}{1.33} \cdot \frac{887270.0}{288} = 785.6 \text{ K}$$

$$p^*_{td} := p^*_{ti} \cdot \left(1 - \frac{T^*_{ti} - T^*_{td}}{T^*_{ti} \cdot \eta^*_t}\right)^{\frac{k_g}{k_g - 1}} = 3096000 \cdot \left(1 - \frac{1550 - 785.6}{1550 \cdot 0.9}\right)^{\frac{1.33}{1.33 - 1}} = 126203.0 \text{ Pa}$$

8. The gas parameters determination at the exit from the primary flow jet nozzle (station jnI)

We determine actual jet nozzle pressure ratio of the primary flow π_{jnI} and compare it with critical jet nozzle presuure ratio at the jet nozzle π_{jncrI} by the formulas:

$$\pi_{jnI} := \frac{p^*_{td}}{p_{am}} = \frac{126203.0}{101325} = 1.246 = 1.246$$

$$\pi_{jncrI} := \left(\frac{k_g + 1}{2}\right)^{\frac{k_g}{k_g - 1}} = \left(\frac{1.33 + 1}{2}\right)^{\frac{1.33}{1.33 - 1}} = 1.851 = 1.851$$

As $\pi_{jnI} < \pi_{jncrI}$ full expansion takes place in the jet nozzle of the engine primary flow $p_{jnI} = p_{am}$ and jet velocity of gas from jet nozzle is determined by the formula, where φ.jnI=0.975 is velocity coefficient of the primary flow jet nozzle:

$$c_{jnI} := \varphi_{jnI} \cdot \sqrt{2 \cdot \frac{k_g}{k_g - 1} \cdot R_g \cdot T^*_{td} \cdot \left[1 - \left(\frac{p_{am}}{p^*_{td}}\right)^{\frac{k_g - 1}{k_g}}\right]}$$

$$c_{jnI} = 303.2 \ \frac{m}{s}$$

The static air temperature in the section jnI is found by the formula:

$$T_{jn} := T^*_{td} - \frac{k_g - 1}{k_g} \cdot \frac{c_{jnI}^2}{2 \cdot R_g} = 785.6 - \frac{1.33 - 1}{1.33} \cdot \frac{303.2^2}{2 \cdot 288} = 746.0 \text{ K}$$

9. The engine main specific parameters and mass air flow rate determination

Specific thrust is determined by the following equations, N*s/kg:

$$P_{spI} := c_{jnI} \cdot \left(1 + g_f\right) = 303.2 \cdot (1 + 0.02118) = 309.6 = 309.6$$

$$P_{spII} := c_{jnII} = 294.5$$

$$P_{sp} := \frac{P_{spI} + m \cdot P_{spII}}{1 + m} = \frac{309.6 + 6 \cdot 294.5}{1 + 6} = 296.7 = 296.7$$

The specific fuel consumption is, kg/(N*h):

$$C_{sp} := \frac{3600 \cdot g_f \cdot \left(1 - g_{cool}\right)}{P_{sp} \cdot (1 + m)} = \frac{3600 \cdot 0.02118 \cdot (1 - 0.027)}{296.7 \cdot (1 + 6)} = 0.03572 = 0.036$$

The mass air flow rate through engine as a whole G_a, the mass aie flow rate through the inner duct G_{aI} and through the outer duct G_{aII} are found by the following equations:

$$G_a := \frac{P}{P_{sp}} = \frac{111000}{296.7} = 374.1 = 374.1 \ \frac{kg}{s}$$

$$G_{aI} := \frac{G_a}{1 + m} = \frac{374.1}{1 + 6} = 53.44 = 53.44 \ \frac{kg}{s}$$

$$G_{aII} := \frac{m}{1 + m} \cdot G_a = \frac{6}{1 + 6} \cdot 374.1 = 320.7 = 320.7 \ \frac{kg}{s}$$

The internal engine efficiency is:

$$\eta_{in} := \frac{P_{spI}^2 + m \cdot P_{spII}^2}{2 \cdot g_f \cdot H_u \cdot \left(1 - g_{cool}\right)} = \frac{309.6^2 + 6 \cdot 294.5^2}{2 \cdot 0.02118 \cdot 43 \cdot 10^6 \cdot (1 - 0.027)} = 0.3477 = 0.348$$

2.4 The gas-dynamic calculation

1. The fan inlet diametric dimensions determination

Taking into account a comparatively big mass air flow rate and in order to reduce the engine diametrical sizes we set:

axial air speed c_{1a}=200 m/s

fan tip circumferential velocity u_{1ft} = 450 m/s

relative diameter of the first stage fan sleeve d_1=0.3

Determine air flow reduced velocity λ_{1a} by the formula:

$$\lambda_{1a} = \frac{c_{1a}}{18.3 \cdot \sqrt{T^*_{fi}}} = \frac{200}{18.3 \cdot \sqrt{288.1}} = 0.6439 = 0.644$$

Relative density of air flux can be determined by the formula:

$$q_{(\lambda 1a)} := \left(\frac{k+1}{2}\right)^{\frac{1}{k-1}} \cdot \lambda_{1a} \cdot \left(1 - \frac{k-1}{k+1} \cdot \lambda_{1a}^2\right)^{\frac{1}{k-1}} = \left(\frac{1.4+1}{2}\right)^{\frac{1}{1.4-1}} \cdot 0.6439 \cdot \left(1 - \frac{1.4-1}{1.4+1} \cdot 0.6439^2\right)^{\frac{1}{1.4-1}}$$

$$q_{(\lambda 1a)} = 0.849$$

The fan inlet area is, where m_a=0.040348 kg*K/J:

$$F_{fi} := \frac{G_a \cdot \sqrt{T^*_{fi}}}{m_a \cdot p^*_{fi} \cdot q_{(\lambda 1a)}} = \frac{374.1 \cdot \sqrt{288.1}}{0.040348 \cdot 100818 \cdot 0.8492} = 1.838 \ m^2$$

The fan external diameter at the inlet in the first stage is calculated by the formula:

$$D_{1ft} := \sqrt{\frac{4 \cdot F_{fi}}{\pi \cdot \left(1 - d_1^2\right)}} = \sqrt{\frac{4 \cdot 1.838}{\pi \cdot \left(1 - 0.3^2\right)}} = 1.604 = 1.604 \ m$$

Expressing in round numbers the obtained external diameter D_{1ft} we can calculate sleeve diameter:

$$D_{1sl} := \sqrt{D_{1ft}^2 - \frac{4 \cdot F_{fi}}{\pi}} = \sqrt{1.604^2 - \frac{4 \cdot 1.838}{\pi}} = 0.4823 = 0.482 \ m$$

Diameter of conditional section aeparating the primary and secondary air flows is determined as follows:

$$D_1 := \sqrt{D_{1ft}^2 - \frac{4}{\pi} \cdot \frac{G_{aII}}{G_a} \cdot F_{fi}} = \sqrt{1.604^2 - \frac{4}{\pi} \cdot \frac{320.7}{374.1} \cdot 1.838} = 0.7528 = 0.753 \text{ m}$$

2. Determination of turbofan engine fan stages number

Setting u_{1ft}=550 m/s circumferential velocity on diameter D1 is determined as:

$$u_I := u_{1ft} \cdot \frac{D_1}{D_{1ft}} = 550 \cdot \frac{0.8}{1.604} = 274.3 = 274.3 \ \frac{m}{s}$$

$$u_{sl} := u_{1ft} \cdot \frac{D_{1sl}}{D_{1ft}} = 550 \cdot \frac{0.4823}{1.604} = 165.4 = 165.4 \ \frac{m}{s}$$

The lattice density near sleeve is assumed as $b/t_{sl} := 2.2$

Determine the lattice density, air twisting in rotor blades and work imparted to the air by the fan blades on the diameter D_1:

$$b/t_I := b/t_{sl} \cdot \frac{D_1}{D_{1ft}} = 2.2 \cdot \frac{0.8}{1.604} = 1.097 = 1.097$$

$$\Delta W_{u1} := c_{1a} \cdot \frac{1.55}{1 + \frac{1.5}{b/t_I}} = 200 \cdot \frac{1.55}{1 + \frac{1.5}{1.097}} = 130.9 = 130.9 \ \frac{m}{s}$$

$$\Delta W_{usl} := c_{1a} \cdot \frac{1.55}{1 + \frac{1.5}{b/t_{sl}}} = 200 \cdot \frac{1.55}{1 + \frac{1.5}{2.2}} = 184.3 = 184.3 \ \frac{m}{s}$$

$$L_1 := u_I \cdot \Delta W_{u1} = 274.3 \cdot 130.9 = 35905.0 = 35905 \text{ J}$$

$$L_{sl} := u_{sl} \cdot \Delta W_{usl} = 165.4 \cdot 184.3 = 30483.0 = 30483 \text{ J}$$

$$L_{fanI} := \frac{1}{2}\left(L_1 + L_{sl}\right) = \frac{1}{2} \cdot (35905 + 30483) = 33194.0 = 33194 \text{ J}$$

3. Distribution of compression work among compressor spools and determination of the number of high and low pressure turbine stages of turbofan engines

To check up the possibility of making a fan in the primary flow zone without booster compressor stages determination the work of high-pressure and low-pressure compressors and the work of high-pressure and low-pressure turbines:

$$L_{HPC} := 0.75 \cdot L_c = 0.75 \cdot 562971 = 422228.0 = 422228 \quad J$$

$$L_{HPT} := \frac{L_{HPC}}{(1 + g_f) \cdot (1 - g_{cool}) \cdot \eta_m} = \frac{422228}{(1 + 0.02118) \cdot (1 - 0.027) \cdot 0.995} = 427079.0 = 427079 \quad J$$

Let $Y^*_{HPT} = 0.49$, when HPT have got 1 stage ($z_{hpt} = 1$, $\eta_{hpt} = 0.89$) pereferial velocity can be determined as:

$$u_{hpt} := Y^*_{HPT} \cdot \sqrt{\frac{2 \cdot L_{HPT}}{z_{hpt} \cdot \eta_{hpt}}} = 0.49 \cdot \sqrt{\frac{2 \cdot 427079}{0.89}} = 480.0 = 480 \quad \frac{m}{s}$$

Work of HPT is performed by one stage, so:

$$L_{st1hpt} := L_{HPT} = 427079 \quad J$$

Work of LPC:

$$L_{LPC} := L_c - L_{HPC} - L_{fanI} = 562971 - 422228 - 33194 = 107549.0 = 107549 \quad J$$

4. Determination of air parameters and diametric dimensions at the fan exit

Assuming $\eta^*_{lpc} = 0.88$, the pressure air in the low-pressure compressor is calculated by the equation:

$$\pi^*_{lpc} := \left[1 + \frac{(L_{LPC} + L_{fanI}) \cdot \eta^*_{lpc}}{\frac{k}{k-1} \cdot R \cdot T^*_{fi}}\right]^{\frac{k}{k-1}} = \left[1 + \frac{(107549 + 33194) \cdot 0.88}{\frac{1.4}{1.4-1} \cdot 287 \cdot 288.1}\right]^{\frac{1.4}{1.4-1}} = 3.48 = 3.48$$

The total air temperature is

$$T^*_{lpcd} := T^*_{fi} + \frac{k-1}{k} \cdot \frac{L_{LPC} + L_{fanI}}{R} = 288.1 + \frac{1.4-1}{1.4} \cdot \frac{107549 + 33194}{287} = 428.2 = 428.2 \quad K$$

The total air pressure is

$$p^*_{lpcd} := p^*_{fi} \cdot \pi^*_{lpc} = 100818 \cdot 3.48 = 350846.0 = 350846 \quad Pa$$

For the turbofan engine with a fan without added compressor stages we assume where $c_{afan2} := c_{inII} - 10 = 294.5 - 10 = 284.5 = 284.5$ m/s

The fan outlet air speed in the primary flow

$$c_{afan1} := c_{1a} - 10 = 200 - 10 = 190.0 = 190 \text{ m/s}$$

The reduced speed velocity of the secondary flow:

$$\lambda_{a\,fanII} := \frac{c_{afan2}}{18.3\sqrt{T^*_{fdII}}} = \frac{284.5}{18.3 \cdot \sqrt{340.2}} = 0.8429 = 0.843$$

$$q(\lambda_{a).fanII} := \left(\frac{k+1}{2}\right)^{\frac{1}{k-1}} \cdot \lambda_{a\,fanII} \cdot \left(1 - \frac{k-1}{k+1} \cdot \lambda_{a\,fanII}^2\right)^{\frac{1}{k-1}} = 0.97($$

The reduced speed velocity of the primary flow:

$$\lambda_{a\,fanI} := \frac{c_{1a}}{18.3\sqrt{T^*_{fdII}}} = \frac{200}{18.3 \cdot \sqrt{340.2}} = 0.5925 = 0.593$$

$$q(\lambda_{a).fanI} := \left(\frac{k+1}{2}\right)^{\frac{1}{k-1}} \cdot \lambda_{a\,fanI} \cdot \left(1 - \frac{k-1}{k+1} \cdot \lambda_{a\,fanI}^2\right)^{\frac{1}{k-1}} = 0.8038$$

The area of the fan exit:

$$F_{fanII} := \frac{G_{aII} \cdot \sqrt{T^*_{fdII}}}{m_a \cdot p^*_{fdII} \cdot q(\lambda_{a).fanII}} = \frac{320.7 \cdot \sqrt{340.2}}{0.040348 \cdot 166349 \cdot 0.9703} = 0.9083 = 0.908 \text{ m}^2$$

The area of the jet nozzle exit:

$$F_{fanI} := \frac{G_{aI} \cdot \sqrt{T^*_{fdII}}}{m_a \cdot p^*_{fdII} \cdot q(\lambda_{a).fanI}} = \frac{53.44 \cdot \sqrt{340.2}}{0.040348 \cdot 166349 \cdot 0.8039} = 0.1827 = 0.183 \text{ m}^2$$

By accepting external diameter behind the fan being 5% less than the fan inlet external diameter we can determine D_{fanII}

$$D_{fanII} := (0.95) \cdot D_{1ft} = 0.95 \cdot 1.604 = 1.524 = 1.524 \text{ m}$$

The diameter of the phantom section dividing the primary and secondary air flows:

$$D_{II} := \sqrt{D_{fanII}^{2} - \frac{4}{\pi} \cdot F_{fanII}} = \sqrt{1.524^{2} - \frac{4}{\pi} \cdot 0.9083} = 1.08 = 1.08 \quad m$$

Assuming the thickness of a separating ring equal to 15mm we can determine outer diameter of the secondary flow as:

$$D_{fanI} := D_{II} - 0.015 = 1.08 - 0.015 = 1.065 = 1.065 \quad m$$

Sleeve diameter can be determined as:

$$D_{fan\ sl} := \sqrt{D_{II}^{2} - \frac{4}{\pi} \cdot F_{fanI}} = \sqrt{1.08^{2} - \frac{4}{\pi} \cdot 0.1827} = 0.9663 = 0.966 \quad m$$

5. Determination of air parameters and diametric sizes at the high-pressure compressor inlet

Air parameters at the inlet to the high-pressure compressor are:

- air temperature $T^*_{a\ hpc} = T^*_{lpcd} = 428.2K$

- air pressure taking into account losses in intermediate casing between the fan and the high-pressure compressor, where $\sigma = 0.98$:

$$p^*_{f\ hpc} = p^*_{lpcd} \cdot \sigma = 350846 \cdot 0.98 = 343829.0\ Pa$$

Reduced velocity, relative density can be determined:

$$\lambda_{a\ hpc} := \frac{c_{a\ hpc}}{18.3\sqrt{T^*_{lpcd}}} = \frac{200}{18.3 \cdot \sqrt{428.2}} = 0.5281 = 0.528$$

Where $c_{a\ hpc} := c_{afanI} + 10 = 200 \ m/s$

$$q(\lambda_{a).hpc} := \left(\frac{k+1}{2}\right)^{\frac{1}{k-1}} \cdot \lambda_{a\ hpc} \cdot \left(1 - \frac{k-1}{k+1} \cdot \lambda_{a\ hpc}^{2}\right)^{\frac{1}{k-1}} = 0.739$$

The fan outlet area in exit of LPC:

$$F_{a\,hpc} := \frac{G_{aI} \cdot \sqrt{T^*_{lpcd}}}{m_a \cdot p^*_{lpcd} \cdot q(\lambda_{a).hpc}} = \frac{53.44 \cdot \sqrt{428.2}}{0.040348 \cdot 350846 \cdot 0.7396} = 0.1056 = 0.106 \text{ m}$$

Relative diameter of the working wheel (WW) at the entrance to the high-pressure compressor is assumed as $d_b = 0.8$ and external diameter D_{1hpc} is determined as:

$$D_{1hpc} := \sqrt{\frac{4 \cdot F_{a\,hpc}}{\pi\left(1 - d_b^{\,2}\right)}} = \sqrt{\frac{4 \cdot 0.1056}{\pi \cdot \left(1 - 0.8^2\right)}} = 0.6111 = 0.611 \text{ m}$$

The first stage WW sleeve diameter of a high-pressure compressor is determined as:

$$D_{a\,hpc\,sl} := \sqrt{D_{1hpc}^{\,2} - \frac{4}{\pi} \cdot F_{a\,hpc}} = \sqrt{0.6111^2 - \frac{4}{\pi} \cdot 0.1056} = 0.4889 = 0.489 \text{ m}$$

The height of the WW blade at the entrance to the high-pressure compressor is determined as:

$$h_{a\,hpc} := \frac{D_{1hpc} - D_{a\,hpc\,sl}}{2} = \frac{0.6111 - 0.4889}{2} = 0.0611 = 0.061 \text{ m}$$

6. Determination of air parameters and diametric sizes at the high-pressure compressor exit

At first we determine more exactly air parametrs at the HPC exit. According to the thermodynamic calculation the pressure $p^*_{cd} = 3159000$ Pa. The HPC work $L_{HPC} = 422228$ Pa. Air temperaturebeyond the HPC is determined by the formula:

$$T^*_{hpc} := T^*_{lpcd} + \frac{k - 1}{k} \cdot \frac{L_{HPC}}{R} = 428.2 + \frac{1.4 - 1}{1.4} \cdot \frac{422228}{287} = 848.5 = 848.5 \text{ K}$$

The pressure ratio in HPC is calculated by the equation:

$$\pi^*_{hpc} := \frac{p^*_{cd}}{p^*_{lpcd}} = \frac{3159000}{350846} = 9.004 = 9.004$$

Assuming that air speed at the exit of high-pressure compressor is determined as $c_{hpc} = 140$ m/s, we can determine λ_{1a} and $q(\lambda)_{1a}$ by the formula:

$$\lambda_{hpc} := \frac{c_{hpc}}{18.3\sqrt{T^*_{hpc}}} = \frac{140}{18.3 \cdot \sqrt{848.5}} = 0.2626 = 0.263$$

$$q(\lambda)_{hpc} := \left(\frac{k+1}{2}\right)^{\frac{1}{k-1}} \cdot \lambda_{hpc} \cdot \left(1 - \frac{k-1}{k+1} \cdot \lambda_{hpc}^{2}\right)^{\frac{1}{k-1}} = 0.4024$$

The cross-section area at the high-pressure compressor exit is determined as:

$$F_{hpc} := \frac{G_{aI} \cdot \sqrt{T^*_{hpc}}}{m_a \cdot p^*_{cd} \cdot q(\lambda)_{hpc}} = \frac{53.44 \cdot \sqrt{848.5}}{0.040348 \cdot 3159000 \cdot 0.4024} = 0.03035 = 0.03 \text{ m}$$

Relative diameter of the working wheel (WW) at the exit of the high-pressure compressor is assumed as $d_b = 0.9$ and external diameter D_{2hpc} is determined as:

$$D_{2hpc} := \sqrt{\frac{4 \cdot F_{hpc}}{\pi\left(1 - d_b^{2}\right)}} = \sqrt{\frac{4 \cdot 0.03035}{\pi \cdot \left(1 - 0.9^{2}\right)}} = 0.451 = 0.451 \text{ m}$$

The last stage WW sleeve diameter of a high-pressure compressor is determined as:

$$D_{2hpc\,sl} := \sqrt{D_{2hpc}^{2} - \frac{4}{\pi} \cdot F_{hpc}} = \sqrt{0.451^{2} - \frac{4}{\pi} \cdot 0.03035} = 0.4059 = 0.406 \text{ m}$$

The height of the WW blade at the exit of the high-pressure compressor is determined as:

$$h_{hpc} := \frac{D_{2hpc} - D_{2hpc\,sl}}{2} = \frac{0.451 - 0.4059}{2} = 0.02255 = 0.023 \text{ m}$$

9. Determination of diametric sizes at the high-pressure turbine entrance

We set the angle of a stream outlet from ND $\alpha = 15°$ and determine jet velocity of gas emission from the ND

$$C_{1hpt} := \frac{L_{st1hpt}}{u_{hpt} \cdot \cos\left(\alpha_1 \cdot \text{deg}\right)} = \frac{427079}{480 \cdot \cos(15 \cdot \text{deg})} = \frac{889.7}{\cos(15.0 \cdot \text{deg})} = 921.085 \ \frac{\text{m}}{s}$$

Reduced velocity, relative density

$$\lambda_{1h} := \frac{C_{1hpt}}{18.3\sqrt{T^*_{ti}}} = \frac{921.08521771085088}{18.3 \cdot \sqrt{1550}} = 1.278 = 1.278$$

$$q(\lambda_{1h}).nd := \left(\frac{k+1}{2}\right)^{\frac{1}{k-1}} \cdot \lambda_{1h} \cdot \left(1 - \frac{k-1}{k+1} \cdot \lambda_{1h}^{2}\right)^{\frac{1}{k-1}} = 0.910947$$

The gas flow rate G_g and the gas pressure at the exit of the turbine nozzle diaphragm (ND), where $\sigma_{nd} = 0.96$, are determined as:

$$G_{g\,hpt} := G_{al} \cdot \left(1 + g_f\right) \cdot \left(1 - g_{cool}\right) = 53.44 \cdot (1 + 0.02118) \cdot (1 - 0.027) = 53.1 = 53.1 \ \frac{kg}{s}$$

$$p^*_{hpt\,nd} := p^*_{cd} \cdot \sigma_{cc} \cdot \sigma_{nd} = 3159000 \cdot 0.98 \cdot 0.96 = 2.972e6 = 2972000 \ \ Pa$$

The cross-setcion area at the ND exit, where $m_g = 0.0396$ is determined by the formula:

$$F_{1hnd} := \frac{G_{g\,hpt} \cdot \sqrt{T^*_{ti}}}{m_g \cdot p^*_{hpt\,nd} \cdot q(\lambda_{1h}).nd \cdot \sin\left(\alpha_1 \cdot deg\right)} = \frac{53.1 \cdot \sqrt{1550}}{0.0396 \cdot 2972000 \cdot 0.91095 \cdot \sin(15 \cdot deg)}$$

$$F_{1hnd} = 0.075 \ \ m^2$$

Asssming that $D_{hpt\,md} = 0.6$ (due to drawing)

Then the length of turbine blade is determined as:

$$h_{hpt} := \frac{F_{1hnd}}{\pi \cdot D_{hpt\,md}} = \frac{0.075}{\pi \cdot 0.6} = 0.03979 = 0.04 \ \ m$$

So the external diameter of turbine entrance is:

$$D_{hpt} := D_{hpt\,md} + h_{hpt} = 0.6 + 0.04 = 0.64 = 0.64 \ \ m$$

After we can determine sleeve diameter

$$D_{hpt\,sl} := \sqrt{D_{hpt}^{2} - \frac{4}{\pi} \cdot F_{1hnd}} = \sqrt{0.64^2 - \frac{4}{\pi} \cdot 0.075} = 0.5605 = 0.561 \ m$$

The axial velocity of the gas at the turbine wheel entrance is determined by the formula:

$$C_{1a\,hpt} := C_{1hpt} \cdot \sin(\alpha_1 \cdot deg) = 921.085 \cdot \sin(15 \cdot deg) = 921.1 \cdot \sin(15.0 \cdot deg)$$

$$C_{1a\,hpt} = 238.398 \ \frac{m}{s}$$

8. Determination of diametric sizes at the high-pressure turbine exit

Gas parameters at the high-pressure turbine exit are determined as:

$$T^*_{hpt} := T^*_{ti} - \frac{L_{HPT}}{\frac{k_g}{k_g - 1} \cdot R_g} = 1550 - \frac{427079}{\frac{1.33}{1.33 - 1} \cdot 288} = 1182.0 = 1182 \ K$$

$$p^*_{hpt} := p^*_{hpt\,nd} \cdot \left(1 - \frac{T^*_{ti} - T^*_{hpt}}{T^*_{ti} \cdot \eta_{hpt}}\right)^{\frac{k_g}{k_g - 1}} = 2972000 \cdot \left(1 - \frac{1550 - 1182}{1550 \cdot 0.89}\right)^{\frac{1.33}{1.33 - 1}} = 851024$$

We set the reduced gas velocity $\lambda_{2a\,hpt} = 0.45$, that corresponds to axial component of gas speed at the high-pressure turbine exit:

$$C_{2a\,hpt} := \lambda_{2a\,hpt} \cdot 18.15 \cdot \sqrt{T^*_{hpt}} = 0.45 \cdot 18.15 \cdot \sqrt{1182} = 280.8 = 280.8 \ \frac{m}{s}$$

$$q(\lambda_{2a)hpt} := \left(\frac{k + 1}{2}\right)^{\frac{1}{k - 1}} \cdot \lambda_{2a\,hpt} \cdot \left(1 - \frac{k - 1}{k + 1} \cdot \lambda_{2a\,hpt}^2\right)^{\frac{1}{k - 1}} = 0.651$$

Taking into account, that part of the cooling iar gets into the gas sream and mixes up with it, we assume $g_{cool2} = 0.01$, and determine the gas flow reate at the high-pressure turbine exit:

$$G_{G\,hpt} := G_{aI} \cdot (1 + g_f) \cdot (1 - g_{cool2}) = 53.44 \cdot (1 + 0.02118) \cdot (1 - 0.01) = 54.03 = 54.03 \ \frac{kg}{s}$$

The cross-section area at the high-pressure turbine exit is determined by the formula:

$$F_{hptd} := \frac{G_{G\,hpt} \cdot \sqrt{T^*_{hpt}}}{m_g \cdot p^*_{hpt} \cdot q(\lambda)_{2a).hpt}} = \frac{54.03 \cdot \sqrt{1182}}{0.0396 \cdot 851024 \cdot 0.6515} = 0.0846 = 0.085 \ m^2$$

Assuming $D_{hptd\,md} = D_{hpt\,md} = 0.6m$ and we determine the height of the blade of the high-pressure turbine first stage

$$h_{hptd} := \frac{F_{hptd}}{\pi \cdot D_{hptd\,md}} = \frac{0.0846}{\pi \cdot 0.6} = 0.04488 = 0.045 \ m$$

Also assuming $D_{hptd} = D_{hpt} = 0.64m$

Then we fing we find HPT sleeve diameter D_{slhptd} as:

$$D_{slhptd} := \sqrt{D_{hptd}^2 - \frac{4}{\pi} \cdot F_{hptd}} = \sqrt{0.64^2 - \frac{4}{\pi} \cdot 0.0846} = 0.5494 = 0.549 \ m$$

9. Determination of high-pressure compressor stages number

The work of the HPC first stage is calculated assuming that the lattice density is $b/t_{sl} := 2.2$

$$\Delta W_{usl} := c_{a\,hpc} \cdot \frac{1.55}{1 + \frac{1.5}{b/t_{sl}}} = 200 \cdot \frac{1.55}{1 + \frac{1.5}{2.2}} = 184.3 = 184.3 \ \frac{m}{s}$$

$$u_{1sl\,hpc} := u_{hpt} \cdot \frac{D_{a\,hpc\,sl}}{D_{hpt}} = 480 \cdot \frac{0.4889}{0.64} = 366.7 = 366.7 \ \frac{m}{s}$$

$$u_{1c\,hpc} := u_{hpt} \cdot \frac{D_{1hpc}}{D_{hpt}} = 480 \cdot \frac{0.6111}{0.64} = 458.3 = 458.3 \ \frac{m}{s}$$

$$L_{st1\,hpc} := u_{1sl\,hpc} \cdot \Delta W_{usl} = 366.7 \cdot 184.3 = 67582.0 = 67582 \ J$$

The work of the HPC last stage is calculated, assuming that the lattice dencity at the sleeve is $b/t_{slz} := 1.8$

$$\Delta W_{uslz} := c_{hpc} \cdot \frac{1.55}{1 + \frac{1.5}{b/t_{slz}}} = 140 \cdot \frac{1.55}{1 + \frac{1.5}{1.8}} = 118.4 = 118.4 \ \frac{m}{s}$$

$$u_{1slz\,hpc} := u_{hpt} \cdot \frac{D_{2hpc\,sl}}{D_{hpt}} = 480 \cdot \frac{0.4059}{0.64} = 304.4 = 304.4 \ \frac{m}{s}$$

$$L_{st1z\,hpc} := u_{1slz\,hpc} \cdot \Delta W_{us1z} = 304.4 \cdot 118.4 = 36040.0 = 36040 \ J$$

The mean work of the stage, J:

$$L_{av\,hpc} := \frac{L_{st1\,hpc} + L_{st1z\,hpc}}{2} = \frac{67582 + 36040}{2} = 51811.0 = 51811$$

The stage number of the HPC is:

$$z_{hpc} := \frac{L_{HPC}}{L_{av\,hpc}} = \frac{422228}{51811} = 8.149$$

Assuming that $z_{hpc} = 9$;

The high-pressure compressor and hgh-pressure turbine power balance is checked by the formula:

$$N_{hpc} := G_{aI} \cdot L_{HPC} = 53.44 \cdot 422228 = 2.256e7 = 22560000 \ W$$
$$N_{hpt} := G_{g\,hpt} \cdot L_{HPT} = 53.1 \cdot 427079 = 2.268e7 = 22680000 \ W$$

Mechanical efficiency

$$\eta_h := \frac{N_{hpc}}{N_{hpt}} = \frac{22560000}{22680000} = 0.9947 = 0.995$$

The rotational speed of high-pressure rotor is determined separately for the compressor and turbines according to the equations:

$$n_{hpc} := \frac{60 \cdot u_{1c\,hpc}}{\pi \cdot D_{1hpc}} = \frac{60 \cdot 458.3}{\pi \cdot 0.6111} = 14323.1 \ rpm$$

$$n_{hpt} := \frac{60 \cdot u_{hpt}}{\pi \cdot D_{hpt}} = \frac{60 \cdot 480}{\pi \cdot 0.64} = 14323 \ rpm$$

10. Determination of the LPT numbers of stages and distribution of work between stages

Taking into account that at the LPT entrance gas temperature $T^*_{lpt}=T^*_{hpt}=1182K$ and consequently LPT need not be cooled, and all the air, cooling components of a MPT, mixes up with the gas flow, we receive

$$G_{g\,lpt} := G_{aI} \cdot \left(1 + g_f\right) = 53.44 \cdot (1 + 0.02118) = 54.57 = 54.57 \ \frac{kg}{s}$$

$$L_{LPT} := \frac{m \cdot L_{fanII} + \left(L_{fanI} + L_{LPC}\right)}{\left(1 + g_f\right) \cdot \eta_m} = \frac{6 \cdot 52370 + 33194 + 107549}{(1 + 0.02118) \cdot 0.995} = 447765.J$$

Taking into account possible gas leakage, we assume $G_{g\,lpt} = 54.57$ kg/s

According to the drawing, received is the scale, of the air flow duct we will determine roughly $D_{lpt\,av} = 0.7$, $u_{1c} = u_{1ft}$, $D_{1c} = D_{1ft}$ then:

$$u_{lpt\,md} := u_{1c} \cdot \frac{D_{lpt\,av}}{D_{1c}} = 550 \cdot \frac{0.7}{1.604} = 240.0 = 240 \ \frac{m}{s}$$

The loading parameter Y* is determined at $z_{lpt} = 4$, $\eta^*_{lpt} = 0.89$

$$Y^* := u_{lpt\,md} \cdot \sqrt{\frac{z_{lpt} \cdot \eta^*_{lpt}}{2 \cdot L_{LPT}}} = 240 \cdot \sqrt{\frac{4 \cdot 0.89}{2 \cdot 447765}} = 0.4785 = 0.479$$

Distribute work between turbine stages, so that work of each next stage was 10-20% less the previous one

$$L_{st1} := \frac{L_{LPT}}{3} = 149255 \ \ J$$

$$L_{st2} := \frac{L_{LPT}}{3} \cdot 0.8 = 119404 \ \ J$$

$$L_{st3} := \frac{L_{LPT}}{3} \cdot 0.7 = 104478.5 \ \ J$$

$$L_{st4} := \frac{L_{LPT}}{3} \cdot 0.5 = 74627.5 \ \ J$$

11. Determination of diametric sizes at the exit of a low-pressure turbine first stage nozzle diaphragm

Assuming angle α = 20°, we can determining ND exhaust gas flow velocity, assuming $C_{2u} = 0$

$$C_1 := \frac{L_{st1}}{u_{lpt\,md} \cdot \cos(\alpha \cdot deg)} = \frac{149255}{240 \cdot \cos(20 \cdot deg)} = \frac{621.9}{\cos(20.0 \cdot deg)} = 661.812 \ \frac{m}{s}$$

$$\lambda_1 := \frac{C_1}{C_{cr}} = \frac{661.8121567027697}{636} = 1.041 = 1.041$$

$$q(\lambda_{1).nd} := 0.9265$$

Axial velocity:

$$C_{1a} := C_1 \cdot \sin(\alpha \cdot deg) = 661.812 \cdot \sin(20 \cdot deg)$$

$$C_{1a} = 226.349 \ \frac{m}{s}$$

The cross-section area at the exit of the LPT ND is determined as :

$$F_{1nd} := \frac{G_{g\,lpt} \cdot \sqrt{T^*_{lpt}}}{m_g \cdot p^*_{hpt} \cdot \sigma_{nd} \cdot q(\lambda_{1).nd} \cdot \sin(\alpha \cdot deg)} = \frac{54.57 \cdot \sqrt{1182}}{0.0396 \cdot 851024 \cdot 0.96 \cdot 0.9265 \cdot \sin(20 \cdot deg)}$$

$$F_{1nd} = 0.183 \ m^2$$

The length of ND stator vane can be determined as:

$$h_{b\,nd} := \frac{F_{1nd}}{\pi \cdot D_{lpt\,av}} = \frac{0.183}{\pi \cdot 0.7} = 0.08322 = 0.083 \ m$$

Then the outer diameter at the exit of the LPT ND is:

$$D_h := D_{lpt\,av} + h_{b\,nd} = 0.7 + 0.08322 = 0.7832 = 0.783 \ m$$

12. Determination of diametric sizes at the exit of a low-pressure turbine exit

The gas parameters at the LPT exit are determined as:

$$T^*_t := T^*_{lpt} - \frac{L_{LPT}}{\frac{k_g}{k_g - 1} \cdot R_g} = 1182 - \frac{447765}{\frac{1.33}{1.33 - 1} \cdot 288} = 796.2 = 796.2 \ K$$

$$p^*_t := p^*_{hpt} \cdot \left(1 - \frac{T^*_{lpt} - T^*_t}{T^*_{lpt} \cdot \eta_{hpt}}\right)^{\frac{k_g}{k_g - 1}} = 851024 \cdot \left(1 - \frac{1182 - 796.2}{1182 \cdot 0.89}\right)^{\frac{1.33}{1.33 - 1}} = 134978\ \text{Pa}$$

We set reduced velocity at the LPT exit $\lambda_{a\,nd} = 0.6$, what coresspond to axial velocity.

$$q(\lambda_a)_{.nd} := \left(\frac{k_g + 1}{2}\right)^{\frac{1}{k_g - 1}} \cdot \lambda_{a\,nd} \cdot \left(1 - \frac{k_g - 1}{k_g + 1} \cdot \lambda_{a\,nd}^2\right)^{\frac{1}{k_g - 1}} = 0.813$$

Cross-sectional area on the exit of the turbine

$$F_t := \frac{G_{g\,lpt} \cdot \sqrt{T^*_t}}{m_g \cdot p^*_t \cdot q(\lambda_t)_{.nd}} = \frac{54.57 \cdot \sqrt{796.2}}{0.0396 \cdot 134978 \cdot 0.9265} = 0.3109 = 0.311\ \text{m}$$

Assuming $D_{lpt\,av} = 0.7$m we determine

$$h_{b\,t} := \frac{F_t}{\pi \cdot D_{lpt\,av}} = \frac{0.3109}{\pi \cdot 0.7} = 0.1414 = 0.141\ \text{m}$$

$$D_t := D_{lpt\,av} + h_{b\,t} = 0.7 + 0.1414 = 0.8414 = 0.841\ \text{m}$$

$$D_{t\,sl} := \sqrt{D_t^2 - \frac{4}{\pi} \cdot F_t} = \sqrt{0.8414^2 - \frac{4}{\pi} \cdot 0.3109} = 0.5587 = 0.559\ \text{m}$$

The fan power and turbine power balance is checked by the formulas:

$$N_{lpt} := G_{g\,lpt} \cdot L_{LPT} = 24434536.05\ \text{W}$$

$$N_{fanI+fan} := G_{aI} \cdot \left(L_{LPC} + L_{fanI}\right) + G_{aII} \cdot L_{fanII} = 24316364.92\ \text{W}$$

$$\eta_{m1} := \frac{N_{fanI+fan}}{N_{lpt}} = \frac{24316364.92}{24434536.05} = 0.995$$

The rotational speed of the LP rotor is determined by the formula:

$$\frac{60 \cdot u_{1c}}{\pi \cdot D_{1c}} = \frac{60 \cdot 550}{\pi \cdot 1.604} = 6549.0\ \text{rpm}$$

$$\frac{60 \cdot u_{lpt\,md}}{\pi \cdot D_{lpt\,av}} = \frac{60 \cdot 240}{\pi \cdot 0.7} = 6548.0\,\text{rpm}$$

13. Determination of turbofan engine jet nozzles diametric sizes

To identify if the primary flow jet nozzle shape is simple convergent or convergent-divergent, we determine the value of jet nozzle differential pressure by the formula, where $\sigma_{jnI} = 0.976$

$$\pi_{jnI} := \frac{p^*_{td} \cdot \sigma_{jnI}}{p_{am}} = \frac{126203.0 \cdot 0.976}{101325} = 1.216$$

The exhaust velocity from the nozzle can be determined as:

$$C_{n1} := \sqrt{2 \cdot \frac{k_g}{k_g - 1} \cdot R_g \cdot T^*_t \cdot \left[1 - \left(\frac{p^*_{am}}{p^*_{td} \cdot \sigma_n}\right)^{\frac{k_g - 1}{k_g}}\right]}$$

$$C_{n1} = 296.1\,\frac{m}{s}$$

Reduced velocity, relative density can be determined:

$$\lambda_{n1} := \frac{C_{n1}}{18.15 \cdot \sqrt{T^*_t}} = \frac{296.1}{18.15 \cdot \sqrt{796.2}} = 0.5782 = 0.578$$

$$q(\lambda)_{n1} := \left(\frac{k_g + 1}{2}\right)^{\frac{1}{k_g - 1}} \cdot \lambda_{n1} \cdot \left(1 - \frac{k_g - 1}{k_g + 1} \cdot \lambda_{n1}^2\right)^{\frac{1}{k_g - 1}} = 0.7929$$

The area and diameter of the nozzle can be determined as:

$$F_{n1} := \frac{G_{g\,lpt} \cdot \sqrt{T^*_t}}{m_g \cdot p^*_t \cdot \sigma_n \cdot q(\lambda)_{n1}} = \frac{54.57 \cdot \sqrt{796.2}}{0.0396 \cdot 134978 \cdot 0.976 \cdot 0.7929} = 0.3723 = 0.372\ m^2$$

$$D_{n1} := \sqrt{\frac{4 \cdot F_{n1}}{\pi}} = \sqrt{\frac{4 \cdot 0.3723}{\pi}} = 0.6885 = 0.688\ m$$

The exhaust velocity from the nozzle of the outer contour is determined in the thermodynamic calculation $C_{n2} = c_{jnII}$. Reduced velocity and relative density of the flow can be determined as:

$$\lambda_{n2} := \frac{C_{n2}}{18.15 \cdot \sqrt{T^*_{fdII}}} = \frac{294.5}{18.15 \cdot \sqrt{340.2}} = 0.8797 = 0.88$$

$$q(\lambda)_{n2} := \left(\frac{k_g + 1}{2}\right)^{\frac{1}{k_g - 1}} \cdot \lambda_{n2} \cdot \left(1 - \frac{k_g - 1}{k_g + 1} \cdot \lambda_{n2}^2\right)^{\frac{1}{k_g - 1}} = 0.9829$$

The area and diameter of the nozzle can be determined as:

$$F_{n2} := \frac{G_{aII} \cdot \sqrt{T^*_{jnII}}}{m_a \cdot p^*_{inII} \cdot \sigma_n \cdot q(\lambda)_{n2}} = \frac{320.7 \cdot \sqrt{340.2}}{0.040348 \cdot 165517 \cdot 0.976 \cdot 0.983} = 0.9232 = 0.923\ m^2$$

The internal diameter of the outer counter exhaust nozzle can be determing using the drawing of the engine $D_{nin} = 1.3$m. Then we can determined the external diameter of this nozzle as:

$$D_{n2} := \sqrt{D_{nin}^2 \cdot \frac{4 \cdot F_{n2}}{\pi}} = \sqrt{1.3^2 \cdot \frac{4 \cdot 0.9232}{\pi}} = 1.409 = 1.409\ m$$

14. Refinement of the engine parameters

In summary of gas-dynamic calculation we find updated caluse of parameters of the designed bypass engine $g_t = 0.0218$. Specific thrust is calculated by the formula, N*s/kg:

$$P_{sp1} := C_{n1} \cdot \left(1 + g_f\right) = 296.1 \cdot (1 + 0.02118) = 302.4 = 302.4$$

$$P_{sp2} := C_{n2} = 294.5 = 294.5 = 294.5$$

$$P_{spz} := \frac{P_{sp1} + m \cdot P_{sp2}}{1 + m} = \frac{302.4 + 6 \cdot 294.5}{1 + 6} = 295.6 = 295.6$$

Engine thrust is determined by the equation

$$P := P_{spz} \cdot G_a = 295.6 \cdot 374.1 = 110583.0 = 110583\ N$$

Specific fuel consumption is calculated as:

$$C_{sp} := \frac{3600 g_t \cdot (1 - g_{cool})}{P_{sp} \cdot (1 + m)} = \frac{3600 \cdot 0.0218 \cdot (1 - 0.027)}{296.7 \cdot (1 + 6)} = 0.03677 \frac{kg}{N \cdot h}$$

2.5 Multi-mode model of the GTE workflow

The flight characteristics of a turbojet engine are one of the types of operational characteristics and consist of speed and altitude characteristics. They make it possible to assess the operational properties of the turbojet engine under various flight conditions and in various modes of its operation.

In view of this, knowledge of the flight characteristics of the engine is very important for flight operation. The thrust generated by the turbojet engine at a certain speed and altitude is the available thrust of the aircraft. The use of this thrust together with the consumed thrust, determined by the aerodynamic drag of the aircraft, makes it possible to determine its flight and tactical data: the most advantageous flight modes, acceleration and deceleration characteristics, altitude, range and duration of flight, etc. In addition, the required degree of engine throttling is determined for level flight at a given speed.

Based on the developed mathematical model of the engine, using the material from [14], you can build a model of throttle-speed characteristics

The graphs (Fig. 2.66) of the set of characteristics of two-shaft turbocharger compressors were approximated on the basis of Appendix 6 [14] and formulas were obtained to optimize the mathematical model and the possibility of using a large number of values.

Formulas for low pressure compressor:

Dependence of the degree of pressure increase on relative speed:

$$\pi_{lpc} = -0{,}0399 n_{rel}^{\,2} + 0{,}7118 n_{rel} + 0{,}3296 \qquad (2.1)$$

Dependence of compressor efficiency on relative revolutions:

$$\eta_{lpc} = 2{,}7886 n_{rel}^{\,3} - 8{,}2074 n_{rel}^{\,2} + 7{,}7496 n_{rel} - 1{,}332 \qquad (2.2)$$

Dependence of air flow rate on relative speed:

$$q(\lambda_{lpc}) = -0{,}3004n_{rel}^{\,2} + 1{,}4708n_{rel} - 0{,}1725 \quad (2.3)$$

Formulas for high pressure compressor:

Dependence of the degree of pressure increase on relative speed:

$$\pi_{hpc} = -3{,}2184n_{rel}^{\,2} + 8{,}2151n_{rel} - 3{,}9967 \quad (2.4)$$

Dependence of compressor efficiency on relative revolutions:

$$\eta_{hpc} = 6{,}3652n_{rel}^{\,3} - 19{,}517n_{rel}^{\,2} + 19{,}744n_{rel} - 5{,}5915 \quad (2.5)$$

Dependence of relative revolutions on air flow coefficient:

$$n_{rel} = 0{,}129q(\lambda_{hpc})^2 + 0{,}1082q(\lambda_{hpc}) + 0{,}7642 \quad (3.6)$$

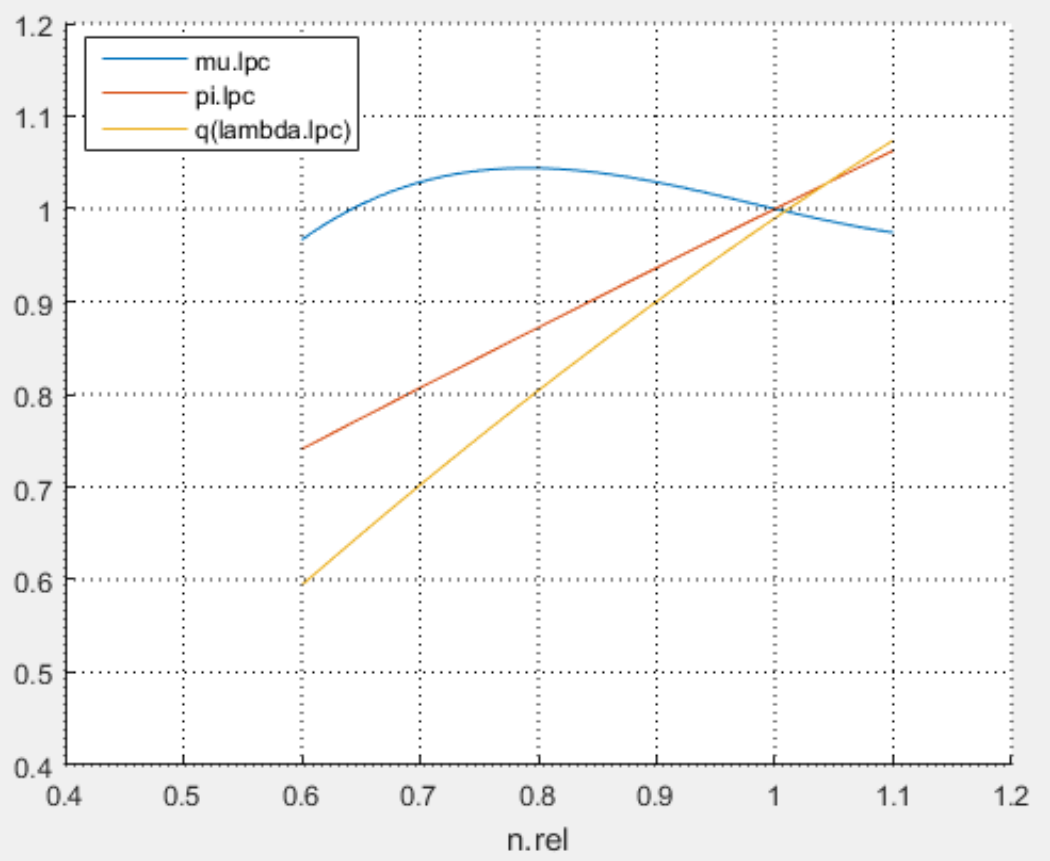

Fig. 2.6 Set of characteristics of TFE LPC

These approximations are an important part of building a mathematical model as it optimizes and makes the model more versatile and flexible. Instead of looking for tabular

values, we will have a ready-made formula for any section or any speed, which perfectly shows the connections between the processes that take place in the turbojet

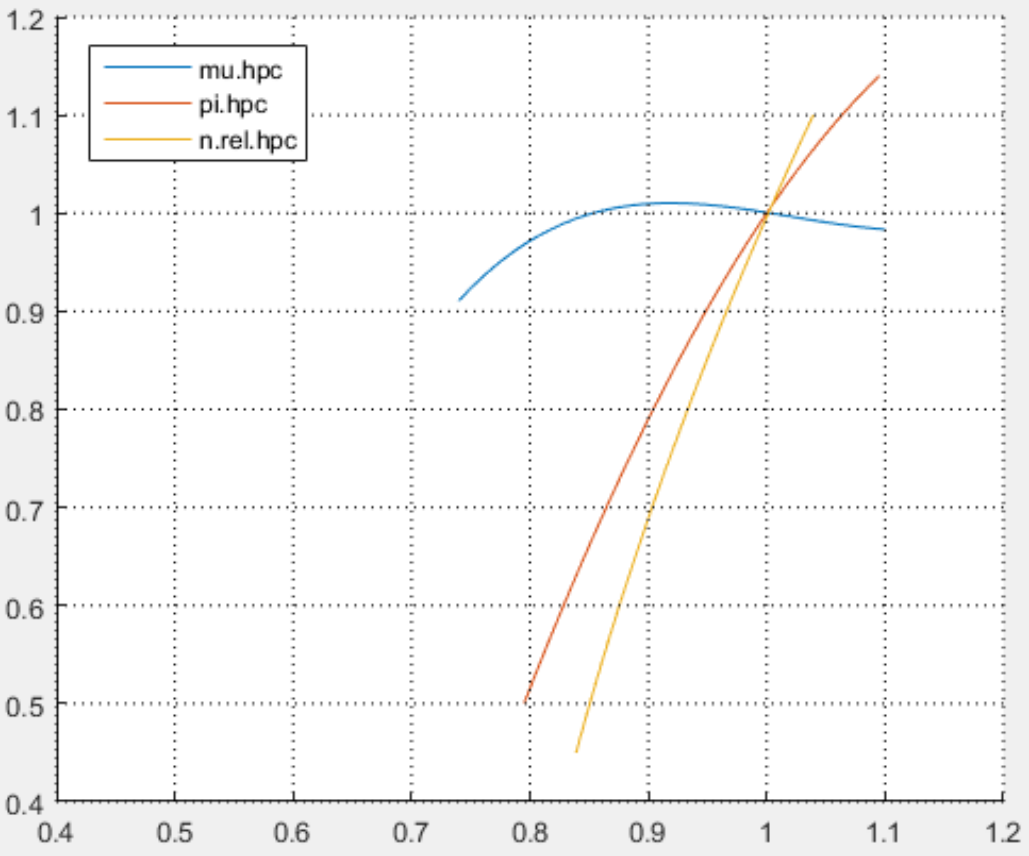

Fig. 2.6 Set of characteristics of TFE HPC

To create a mathematical model that would show us the dependences on the speed of the low-pressure compressor, we first created a linear model that satisfied the mathematical model of the turbojet process. After that, a model was created that could calculate the dependencies between the nodes of the turbojet engine. This created an opportunity to link the environment and the operating parameters of the computing engine

The relative revolutions of the LPC were set as 0.6… 1.1

The results of the multi-mode model depending on the different speeds of the low pressure compressor are shown in Fig.3.3

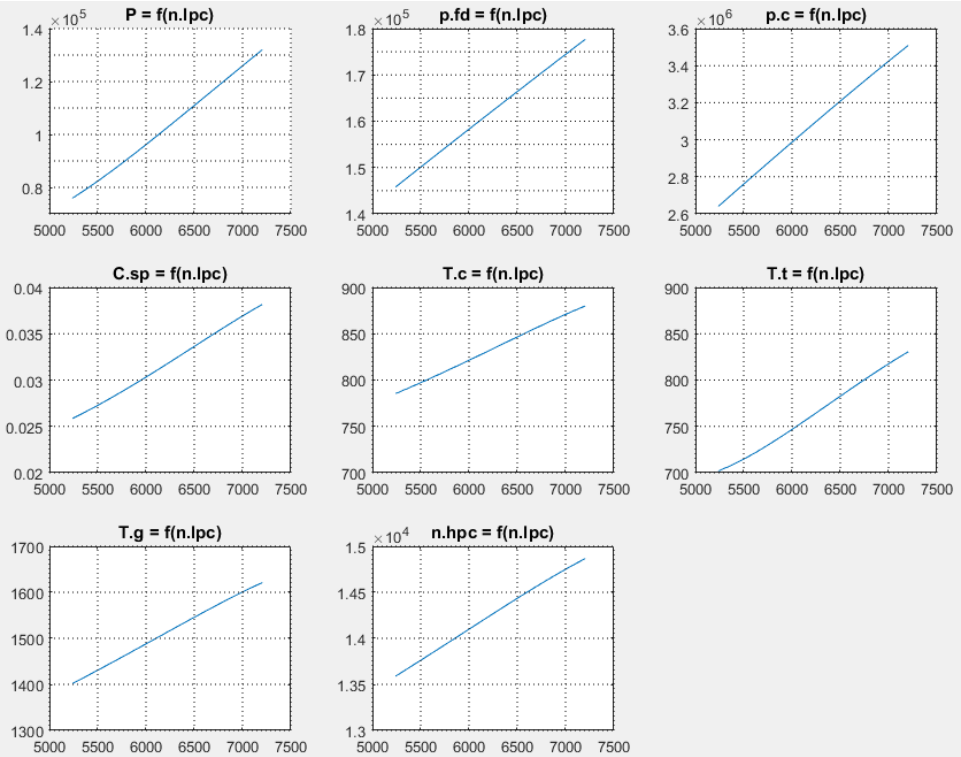

Fig. 2.6 Dependence of engine parameters on LPC rpm

Conclusion to the second chapter:

In this section, we learned what a mathematical model is and what it is important for, namely to reduce the cost of engine development in the future, because with the right mathematical model can replace many experiments that will show the same results as on the stands.

The prototype of the engine, its modular parts were also disassembled, namely:

- Major fan module
- Gas generator module
- LPT module

Also in this section calculations of mathematical model of working process of the settlement engine are shown and on the basis of which served for creation of a multimode model of working processes

3. Method for assessing influence of operating mode and technical state of high-temperature gas turbine engine on the process of damage accumulation in its turbine blades

3.1 Defects tracked

To date, quite a lot of statistics on turbojet engine failures has already been accumulated, in the analysis of which two types of defects can be distinguished, classified by reasons of occurrence: design and production (random deviations in the geometry of the profile, in the technology of manufacturing turbojet engines and their regulation) and operational - irregularity of the air flow with deviation of modes, different operating time of individual blades, and, consequently, wear.

According to statistics from [18], we can see (Fig. 3.1) that most engine failures occur in the rotor of the hot part of the GTE. Also from table 3.1 we can see the statistics of failures of components of different parts of the engine.

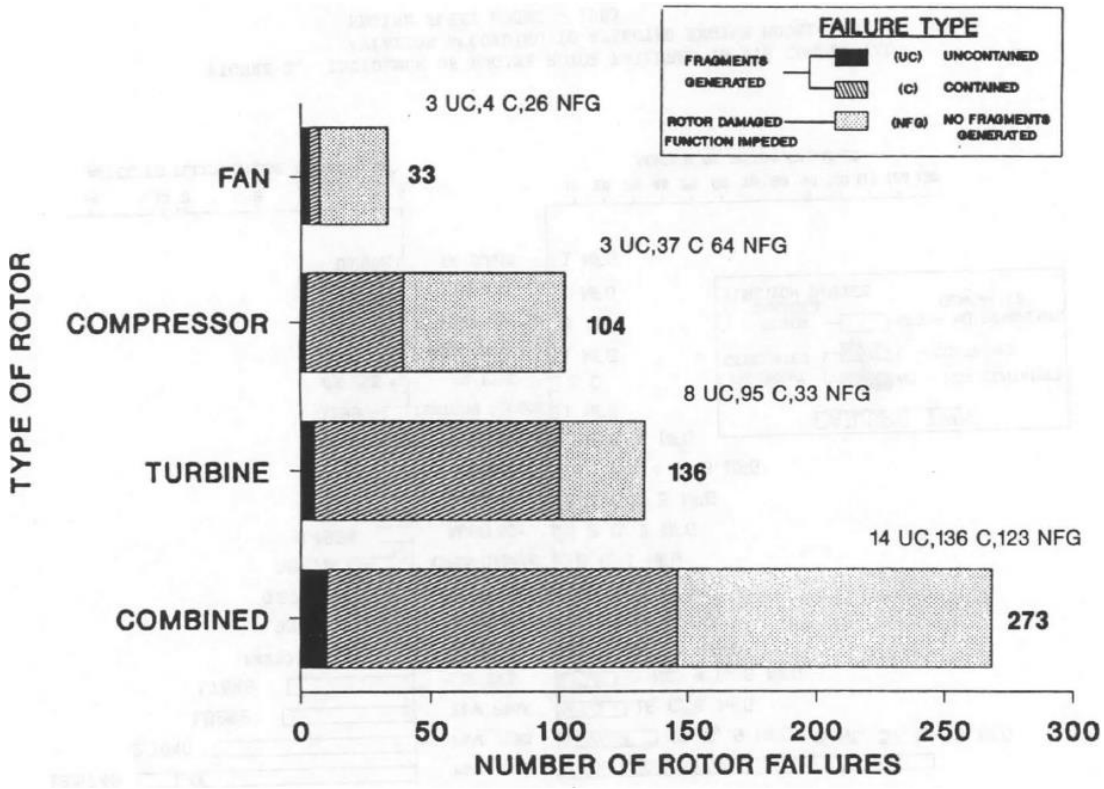

Fig. 3.1 Incidence of engine rotor failures in U.S commercial aviation - 1985

Table 3.1

Статистика відмов по компонентам

ENGINE ROTOR COMPONENTS	TYPE OF FRAGMENT GENERATED									
	DISK		RIM		BLADE		SEAL		TOTAL	
	TF	UCF	TF	UCF	TF	UCF	TF	UCF	TF	UCF
FAN	0	0	0	0	7	3	0	0	7	3
COMPRESSOR	1	1	0	0	39	2	0	0	40	3
TURBINE	5	5	0	0	96	3	2	0	103	8
TOTAL	6	6	0	0	142	8	2	0	150	14

NOTES:
(1) FAILURES THAT PRODUCED FRAGMENTS

TF - TOTAL FAILURES
UCF - UNCONTAINED FAILURES

In Table 3.1 we can see that blade fragments were generated in 142 (95 percent) of the failures; eight (5.3 percent) of these were uncontained[18]. The remaining eight (6 percent) rotor fragment failures were produced by disk and seal[18]. All of the six disk failures were uncontained.

Damage and destruction of the rotor blades and disks of high and low pressure turbines (HPT and LPT) can occur as a result of the following effects

1. Due to the formation of fatigue cracks (Figure 3.2, Figure 3.3). In this case, the main defects of the turbine rotor blades are cracks on the airfoil profile from the side of the trough and back, cracks on the airfoil end face (along the blade axis), cracking at the edge of the perforation holes, surface cracking of the coating on the leading edge of the blade airfoil, spots on the blade airfoil;

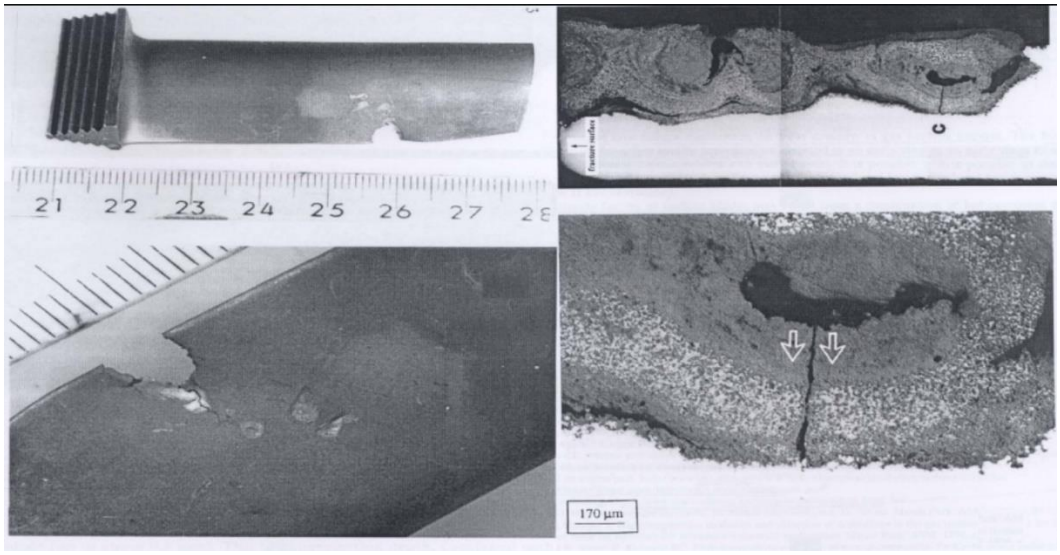

Fig.3.2 Different view of crack on the HPT blade

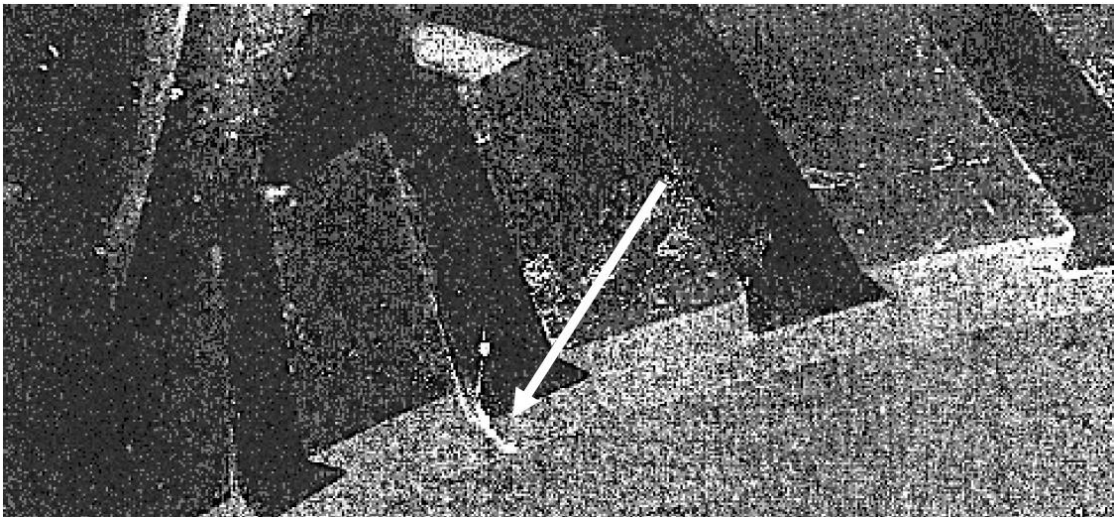

Fig. 3.3 Rim crack

2. Ingress of foreign objects into the flow path (Fig. 3.4). When objects hit, it is possible not only to cause damage, but also with a jump in temperature, they can be completely destroyed, which leads to the loss of subsequent elements, namely disks and blades of the HPT and disks and elements of the injection pump. Such objects can be, burnout of the combustion chamber flame tubes leads to an increase in temperature in front of the HPP, and in some cases, when particles of the flame tube hit the HPT and LPT blades, and to their destruction..

Рис. 3.4**.** LPG blade for gas turbine engine type GTK 10-4 with a nick..

3. In addition, the blades of nozzles and turbine impellers can be destroyed as a result of exceeding the maximum permissible gas temperature. Typical defects in this case are: local chipping, stretching or breakage of a part of the airfoil of the rotor blade, thermal fatigue cracking, burnout of alloying elements of the surface layer, grain growth in blades made of nickel alloys, strong erosion when the protective coating disappears.;

Рис. 3.5 Breakage of a part of the rotor blade of the second stage of the turbine of the Д-30КР-2 engine

4. Part of the damage is due to technological reasons: traces of touching the end of the blade airfoil on the insert, casting defects in the form of cavities and oxide inclusions. The largest number of failures falls on the working blades that have been repaired;

5. Occurring flashing of turbine blades (Figure 3.6) is caused mainly by the ingress of condensate into the fuel gas, and burnouts of cooled hollow blades are caused by irregularities in the operation of their cooling system, sometimes (with built-in combustion chambers) by excessive torch length;

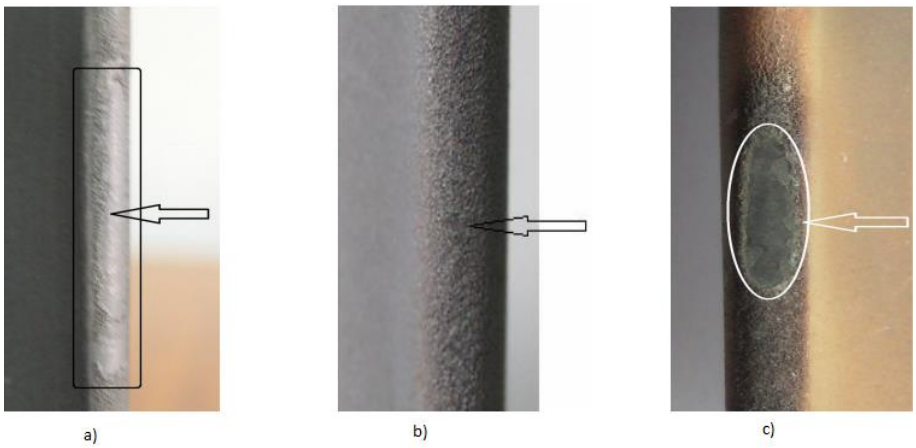

Рис 3.6 Appearance of the turbine rotor blade of the РД33 aircraft gas turbine engine; typical operational damage to its leading edge (indicated by arrows): a - discoloration or peeling of the protective coating; b - local melting of the protective coating; c - destruction of the coating and erosion of the protected alloy

6. Corrosion damage to the blades reduces the endurance limit of their material by 10-30%; therefore, temperature jumps lead to burnout of the blades (Figure 3.7);

Рис. 3.7 Cases of burnout of gas-turbine engine blades, initiated by corrosion damage of the rotor blades of the first stage of the HPE

7. In rare cases, destruction is caused by repeated, periodically repeated thermal stresses during frequent starts and stops of turbines.

Usually, these causes of damage to parts stem from the fact that the loads were exaggerated, and the operating modes did not coincide with those for which the blades were designed. These reasons are also influenced by the previous parts facing the

combustion chamber, HPT and LPT. Namely, their condition and their damage make changes in the further working process of the engine.

Defects of the blade apparatus of an axial compressor by external signs can be divided into two groups

- defects with destruction of the blades. This group includes mechanical damage to the blade apparatus, damage from corrosion and erosion, breakage of blades due to vibration.;

- defects that do not represent clearly pronounced destruction of the scapula. These defects consist in the presence of cracks in the body of the blades or at the leading edge. In many cases, identifying these cracks is difficult and sometimes impossible. Cracks in the blades are usually caused by resonant vibrations of the blades, as a result of which the so-called metal fatigue occurs.

There are several reasons for the failure of axial compressor blades:

1. Damage to the compressor blades by foreign objects entering the flow path. Damage in the form of nicks on the edges of the blades and crushing of the material (Fig. 3.8) become stress concentrators and reduce the vibration strength of the blades. Decreases operational reliability and safety of work. The desire to make the blade edges thinner to reduce losses and improve the fuel efficiency of the turbine makes the problem of blade damage by foreign objects even more urgent.;

Рис. 3.8 Nicks, tears, dents in the fan and compressor blades of the engine CFM56-5B

2. The ingress of natural and industrial dust into the flow path of an axial compressor of a turbojet engine leads to mechanical wear (erosion) and the formation of various kinds of deposits on it. Some types of industrial dust can also corrode the flow path. Erosion leads to a decrease in the service life of the blades, and deposits lead to a deterioration in the aerodynamics of the flow path. Dense deposits of great thickness on the blades of the first stages of the compressor can also cause a change in their vibration characteristics with the appearance of dangerous resonances. In most cases, the destruction of the blades occurs due to their erosive wear, and it is the greater, the greater the concentration of foreign particles.

Their wear is also influenced by the relative position of the guide and working blades of the rotor and stator and the nature of foreign particles. In this case, the leading and trailing edges, the upper part of the rotor blades and the blades of the guide vanes are subject to greater wear. Erosive wear of the blades can also have the appearance of local undercuts.

3. Vibration breakdowns of mainly rotor blades along the root section, sometimes along the cavity of the first tooth, as well as along the peripheral corners. In this case, the fracture is of a fatigue nature. Possible reasons: the appearance of unforeseen disturbing forces, for example, due to local overlap of a part of the guide ring, deviations in maintaining the steps or angles of the guide vanes during manufacture or when replacing the vanes during repair, compressor operation in an unstable (pre-surge) or prohibited by the factory manufacturer's zone, change in vibration characteristics of blades due to erosive wear.

4. Severe rubbing at the ends of the blades can cause bending of the corners at the trailing edge, curvature of the trailing edge itself, as well as fatigue breakages..

5. The blades of an axial compressor fail due to dynamic stresses, the influence of forces from the flow of cyclic air and centrifugal forces from weight acting in all modes of operation of the turbojet engine, low structural reliability of the blade apparatus, deterioration of the surface condition during operation, disturbances in the landings of the blades, disturbances manufacturing technology.

6. Sometimes the destruction of the slots of the blades occurs with their release into the flow path, which leads to a complete failure of the turbojet engine. This occurs during long-term combined action of high static and dynamic stresses together with stress concentrators during overloading of turbines or their long-term operation at rated power modes..

As a rule, the destruction of blades begins with the formation of fatigue cracks, which mainly occur at the trailing edges and, less often, at the input edges. In some cases, cracks form on the back or trough, but only at the tip of the shoulder blades, at the lock.

7. Deviations from the manufacturing technology lead to a violation of the frequency characteristics of the blades, both of the rotor and the stator, which leads to an expansion of the range of resonance modes of the blades and can cause cracking.

8. The formation of cracks can also lead to a flow stall with the formation of vortices at the ends of the blades, due to which oscillations of the blades occur, and the vibration modes can be bending-torsional or plastic depending on the frequencies of the resonant oscillations.

3.2. Damage accumulation model.

To build a model of damage, you must first develop a load model. This model was developed according to the manual [17]

A blade was taken, first for 10 and then for 50 parts to build a model of load propagation. The model considers centrifugal and hot gas loads

Formula for calculating the centrifugal forces that affect any cross section of the HPT blade:

$$\sigma_c = \frac{\rho - u^2}{2}\,(1 - r^2)\,\frac{1+\frac{2*(f-1)}{(1-\nu_{sl})^m(1-r^2)}\left[\frac{(1-r)^{m+1}}{m+1} - \frac{(1-r)^{m+2}}{m+2}\right]}{1+\frac{f-1}{(1-\nu_{sl})^m}(1-r)^m} \qquad (3.1)$$

where σ_c – tensile stress in the design section of the blade, Pa;
ρ – blade material density kg / m3;

u – the peripheral speed of the blade, m / s;

r – relative radius of the blade section, m;

f – the ratio of the areas of the root and end sections of the blade (f = 2 ÷ 4);

m – exponent of the law of variation of the blade sectional area along the radius (m = 2 ÷ 3);

ν – sleeve ratios at the turbine impeller inlet

The stresses from bending by gas forces can be determined exactly by the intensity of gas loads acting on the rotor blade, however, in order to reduce the volume of calculations, it is allowed to accept bending stresses approximately equal to 20-40% of the magnitude of tensile stresses by centrifugal forces in the corresponding sections [17].

$$\sigma_T = 0.2 * \sigma_c \tag{3.2}$$

After calculating the different loads, we can add it to get the total loads

$$\sigma_\Sigma = \sigma_T + \sigma_c \tag{3.3}$$

Then we can see the dependence of loads on the height of the blade (Fig.3.9)

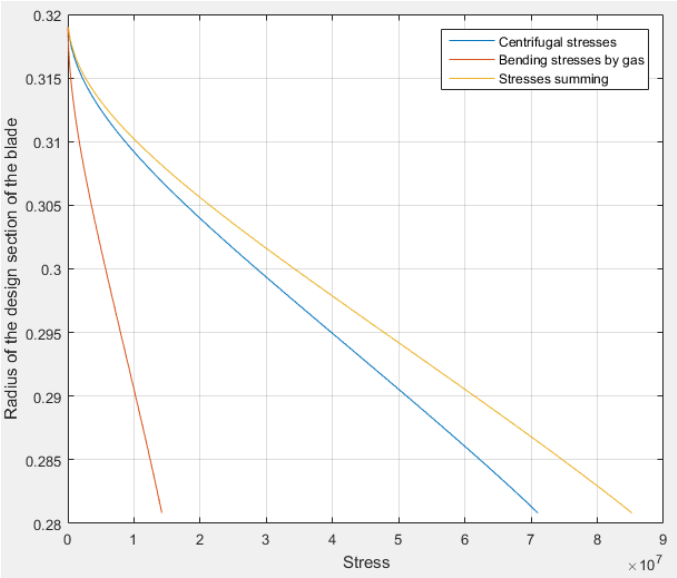

Рис. 3.9 Dependence of stresses on the radius of the design section of the blade

The next step in building a damage model is to find the durability of the blade, or rather its cross sections. Therefore, the Larrson-Miller model [16], which has the form:

$$P_\sigma = T(C + \log(\tau)) \tag{3.4}$$

where $P_\sigma = f(\sigma)$ – Larson-Miller dependence parameter, τ – life time

C – Larson – Miller dependence constant (for the material ЖС26ВСНК accepted C = 20 [20]).

To find long-term strength, we can remake equation 3.4 as follows:

$$\tau(\sigma, T) = 10^{\frac{P_\sigma}{T} - C} \tag{3.5}$$

To determine the temperature on the blade, an approximation was performed, a graph was constructed at 3 points (Fig. 3.10), which indicated the temperature on the blade (root, middle and end section) and a formula was obtained to calculate the temperature at any section:

$$T = -246914r^2 + 148148r - 21042 \tag{3.6}$$

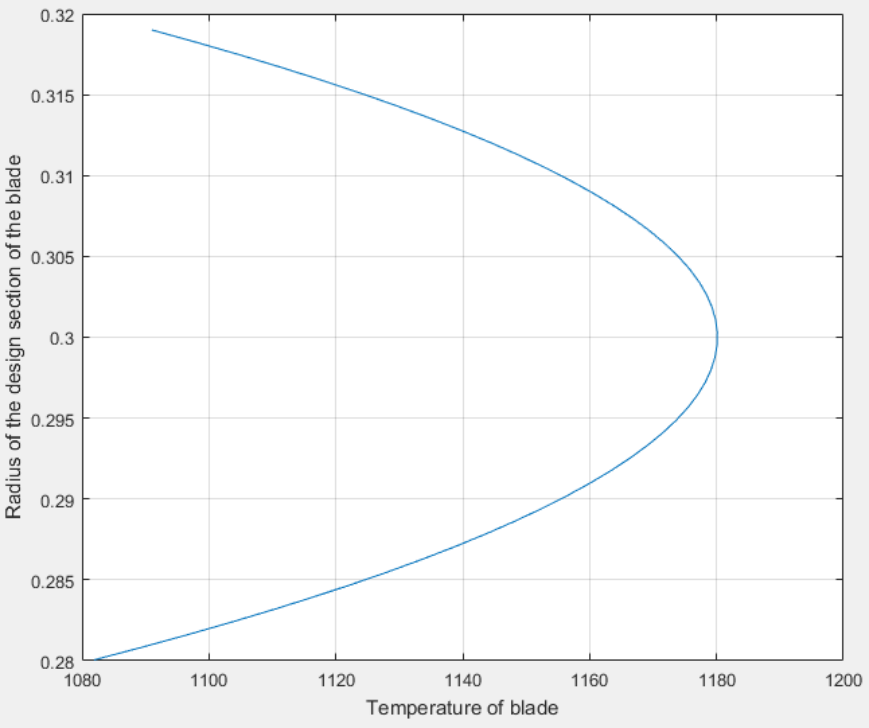

Рис.3.10 Залежність температури від висоти лопатки

And to calculate the Larson-Miller parameter, we took the dependencies on an experimental basis [21], which have the form:

$$P_\sigma = \begin{cases} -34207227 + 7684940 * \lg(\sigma) - 431356 * \lg^2(\sigma) & when \ \lg(\sigma) \geq 8{,}917 \\ -2672855 + 628332 * \lg(\sigma) - 36585 * \lg^2(\sigma) & when \ 8{,}77 \leq \lg(\sigma) < 8{,}917 \\ -67394 + 30235 * \lg(\sigma) - 2260.9 * \lg^2(\sigma) & when \ \lg(\sigma) < 8{,}77 \end{cases} \tag{3.7}$$

Now having all the components we can find out the long-term strength of the blade in its various sections (Fig. 3.11).

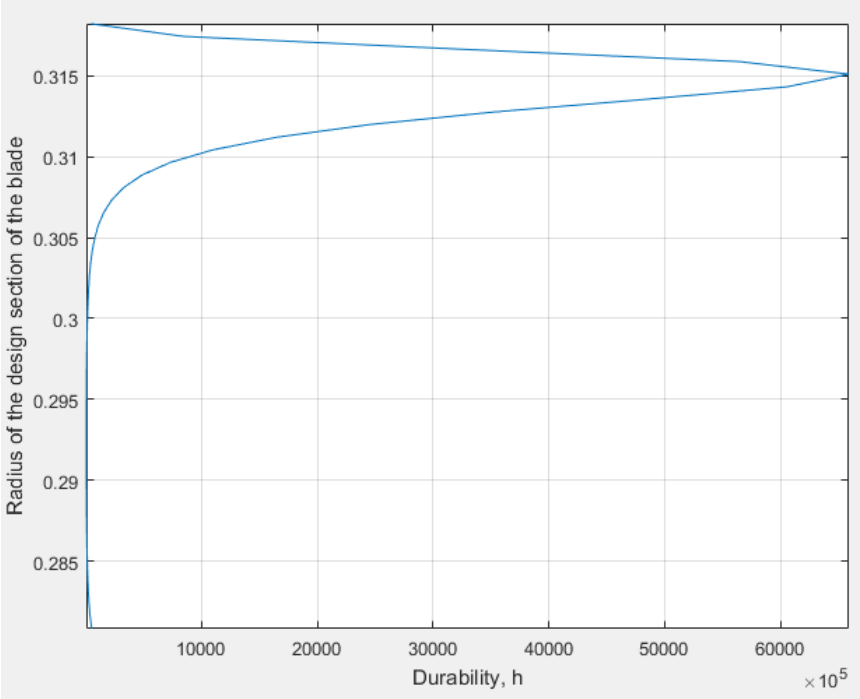

Рис. 3.11 The graph of the durability of different sections of the blade

From the graph it is difficult to see which section has the least durability in the blade, so we will represent the longevity in logarithmic coordinates (Fig. 3.12) which will show that the weakest section of the blade is somewhere 1 \ 3 of the entire height of the blade.

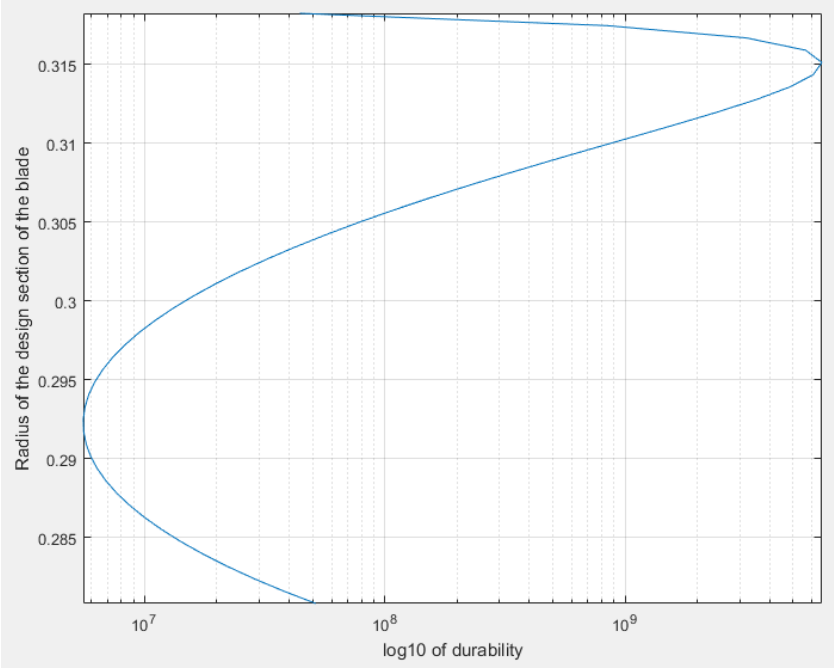

Рис. 3.12 The graph of the durability of different sections of the blade in semi-logarithmic coordinates

Now that we have durability we will be able to count the damage in 1 hour of blade service, the model will look like:

$$\psi = \frac{1}{\tau} \tag{3.8}$$

Thus we get the accumulation of damage to the TVT blade for one hour of engine operation (Fig. 3.13).

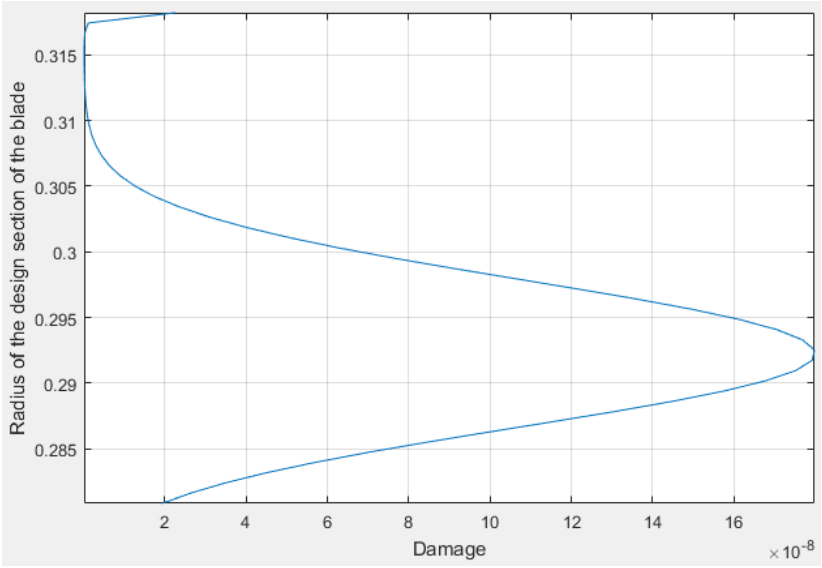

Рис. 3.13 Damage in one hour on different sections of the scapula

From the graph, we are once again convinced of the weakest section of the blade, and it is equal to 0.291 m. It is on this section that the accumulation of damage and the impact of the environment and technical condition on it should be assessed, as this section is a critical section of the entire HPT blade.

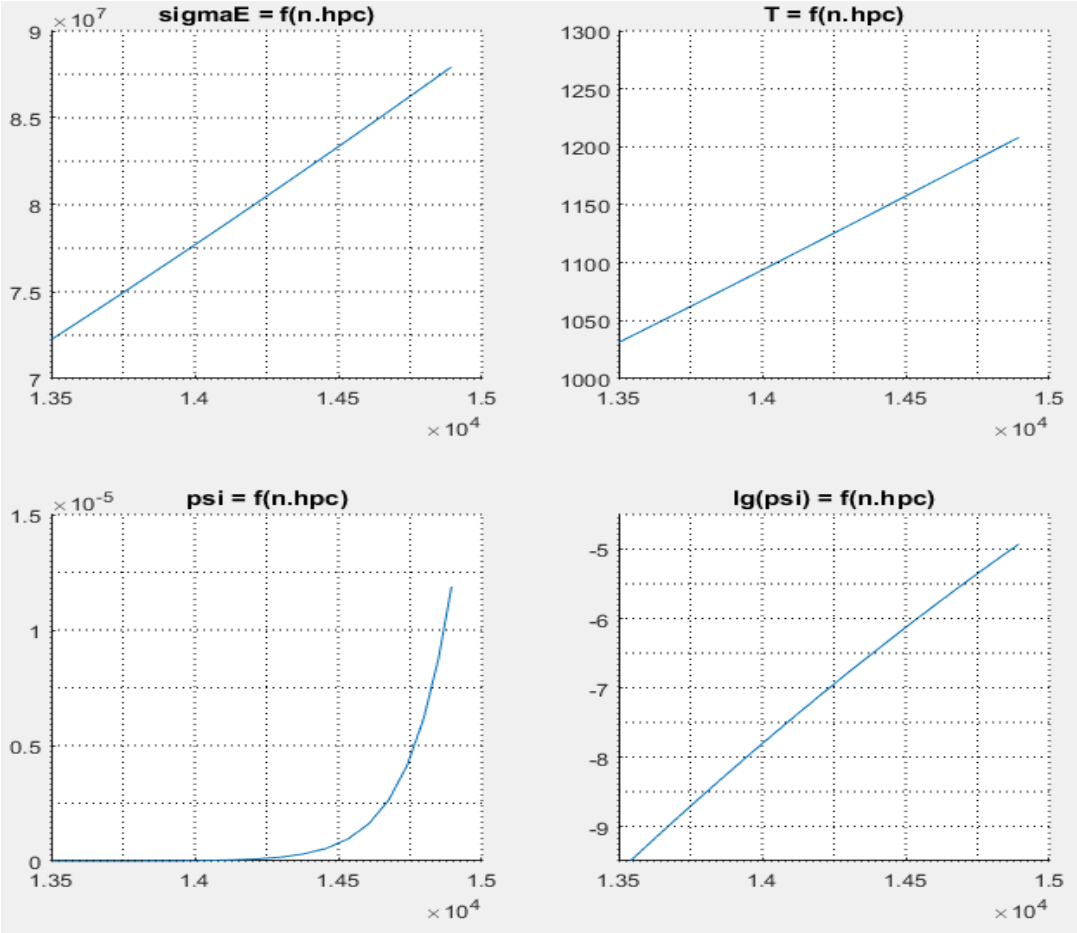

Рис 3.14 Dependences of total loads, blade temperature, accumulation of damage per hour and accumulation of damage in 10 logarithms on HPT rpm

Using the constructed models, the dependences (Fig. 3.14) on the critical section were modeled. We can see how going beyond the calculated modes of operation affects the blade, and how the temperature jump leads the blade to rapid destruction.

Let's increase the ambient temperature by 10 degrees and see how this will affect the accumulation of damage.

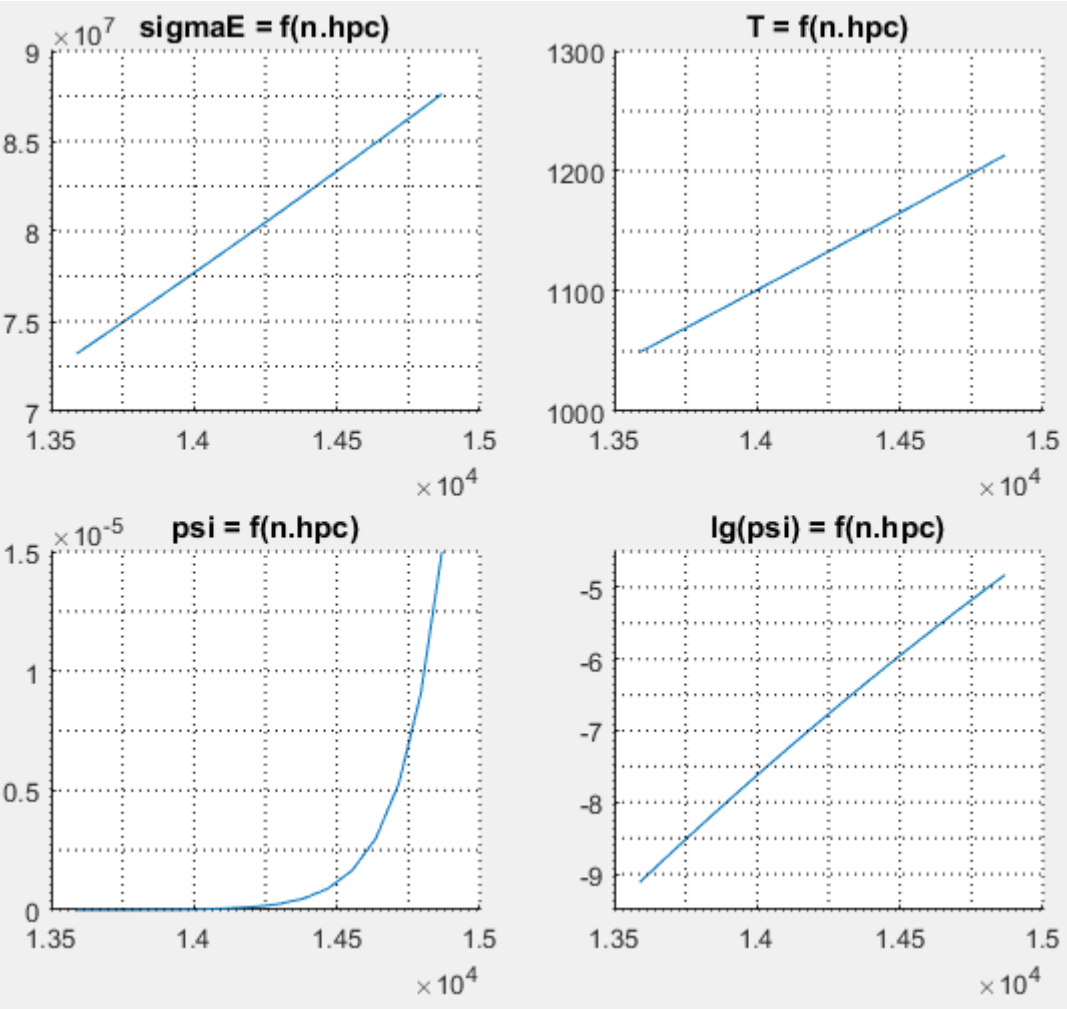

Рис 3. 15 Dependences of total loads, blade temperature, accumulation of damage per hour and accumulation of damage in 10 logarithms on HPT rpm at Tam + 10

We see how an increase in temperature of only 10 degrees leads to an increase in the accumulation of damage by almost an order of magnitude (9.6 times increased accumulation of damage)

Now it is necessary to look at the accumulation of damage under other environmental conditions, namely at an altitude of 1000 m (Fig. 3.16). The air density becomes lower and the damage from this. From the graph we see that the damage is high, but due to the reduced air density the effect of increased temperature decreases.

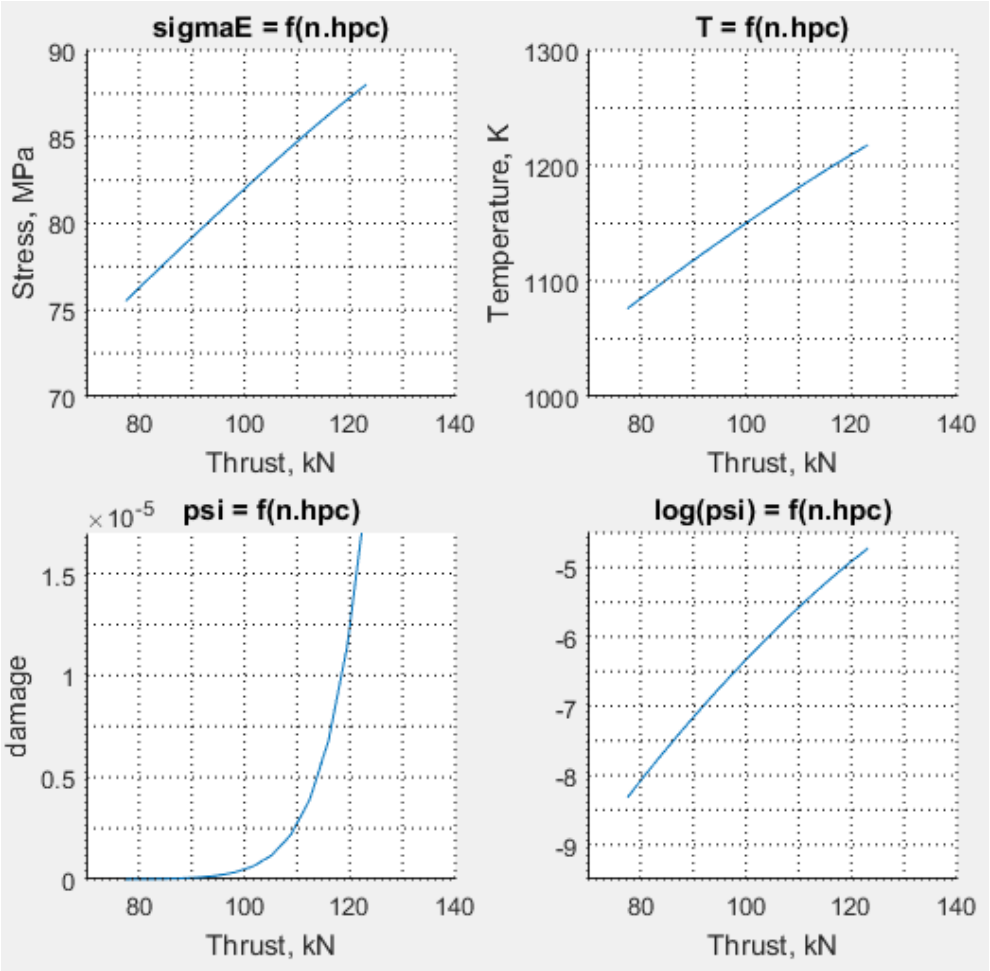

Рис.3.16 Dependences of total loads, blade temperature, accumulation of damage per hour and accumulation of damage in 10 logarithms on the thrust of the engine at H = 1000m

We should not forget about the influence of other parts of the engine on the damage to the blades, from the study [22] we assume that the deterioration of the compressor directly affects its efficiency, so to simulate the deterioration of the compressor we reduce its efficiency by 0.01 and get the result (Fig. 3.17)

From the graph we can see that the accumulation of damage during compressor wear differs by 0.84 units at the maximum design mode. We also see that the wear of the compressor has almost no effect on the load.

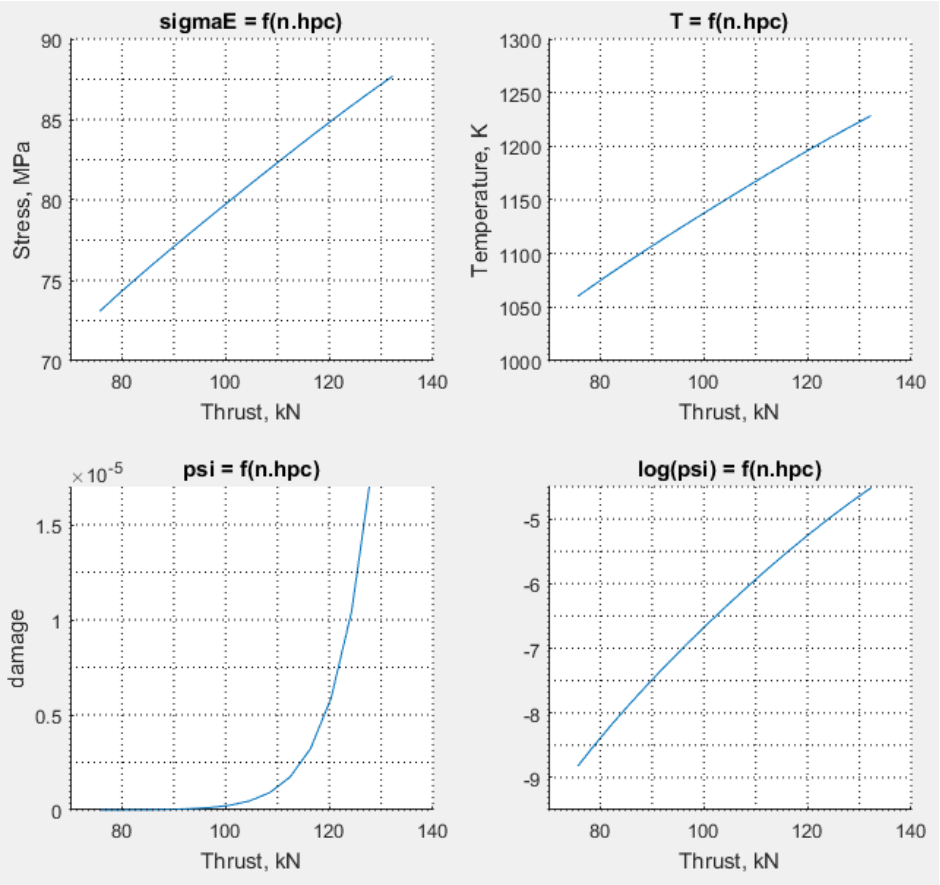

Рис.3.17 Dependences of total loads, blade temperature, damage accumulation per hour and damage accumulation in 10 logarithms on engine thrust during compressor wear

In the next experiment, we will simulate the wear of the fan, in the same way as the compressor, we will reduce its efficiency by 0.01. From the graph (Fig. 3.18) we can see that the wear of the fan has an impact, but compared to the compressor and the environment is much smaller. At the maximum calculated modes of operation, the accumulation is less than 0.01 units. This means that the influence of the fan has the least impact on the accumulation of damage in the blades of HPT TFE.

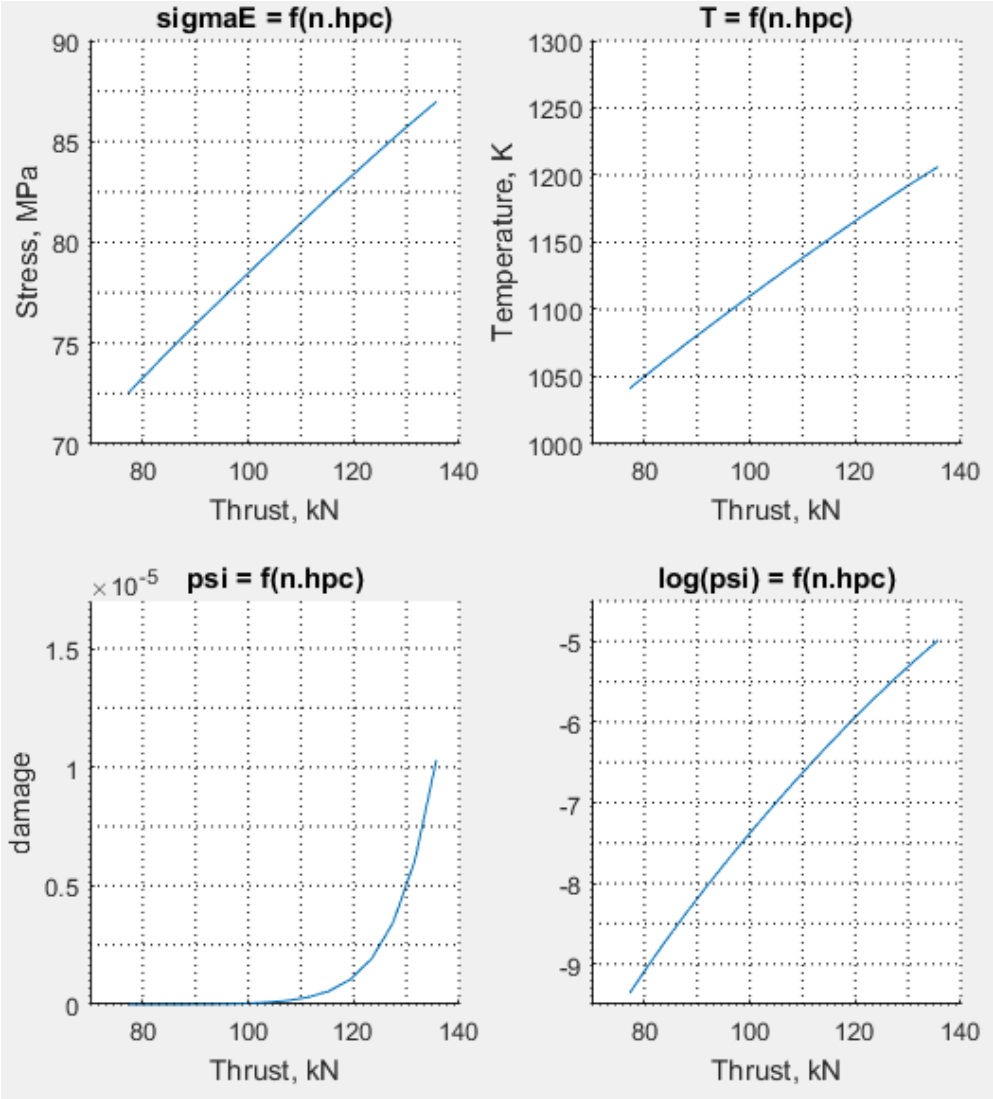

Рис.3.18 Dependencies of total loads, blade temperature, damage accumulation per hour and damage accumulation in 10 logarithms on engine thrust during fan wear

Comparison of all experiments and under standard conditions can be seen in the graph of Fig.3.19

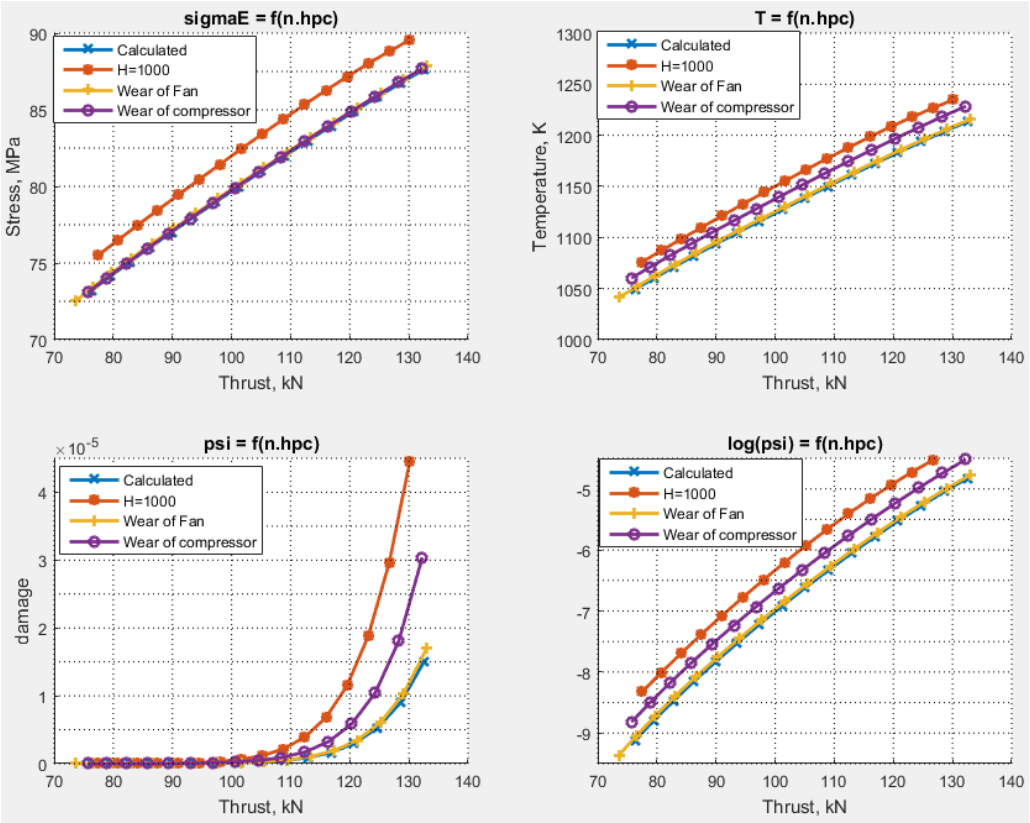

Рис. 3.19 Порівняння експериментів і розрахункових графіків

Conclusion

In this section, damage to the TVT blades was considered, as well as damage to elements that affect the parameters of the workflow, which directly affects the condition of the TVT blades. A damage model was built based on workflow models and elevation characteristics from the previous section,

Experiments were also conducted, based on which it can be concluded that the impact of the environment is much greater than the technical condition of the design engine.

4. Labor Protection

4.1 Introduction

Engineers perform all their calculations and drawings with the help of special software on computers, in specially equipped offices or classrooms, my qualification work is no exception.

In today's world, engineers perform all their calculations and drawings with the help of special software on computers, in specially equipped offices or classrooms, my qualification work is no exception.

The subject of this qualification work is a diagnostic engineer who investigates methods for assessing the impact of the mode of operation and technical condition of a high-temperature gas turbine engine on the process of accumulation of damage in the turbine blades.

In this section, I will look at the working conditions for employees who are constantly conducting their research on computers.

4.2 Analysis of working conditions

In the modern world, scientific and technological progress has seriously changed the conditions of production of engineers, whose work has become more intense and intense, it requires significant mental, emotional and physical energy.

The protection of workers' health, ensuring the safety of working conditions, the elimination of occupational diseases and occupational injuries is one of the main concerns of human society. Attention is drawn to the need for widespread use of progressive forms of scientific organization of labor, minimization of manual, low-skilled labor, the creation of an environment that excludes occupational diseases and occupational injuries.

4.2.1 Workplace organization

The workplace is a space equipped with technical means, where the activities of a diagnostic engineer are carried out

The room where the computers are located should be large enough and well ventilated. Minimum area per computer - 6 m^2 minimum volume - 20 m^3.

The organization of the workplace is a system of measures to equip the workplace with tools and objects of labor and their placement in a certain order. When creating workstations with a computer, the distance between desktops with video monitors should be taken into account, which should be at least 2 m, and the distance between the side surfaces of video monitors - at least 1.2 m.

There are identified 21 spatial parameters for workplace operators, which are presented in Table 4.1 and Figure 4.1.

Table 4.1- Workplace parameters

Spatial parameters	L, mm
1 Seat height	400-500
2 Height of the keyboard from the floor	600-750
3 Keyboard tilt angle	7-15°
4 The width of the main keyboard	not > 400
5 Depth of the main keyboard	not > 200
6 Удаление клавиатуры от края стола	80-100
7 Remove the keyboard from the edge of the table	950-1000
8 Screen tilt angle and normals	0-30°
9 Distance of the screen from the edge of the table	500-700
10 Height of recording surfaces	670-850
11 Recording surface area	600x400
12 Recording Surface Slope of Recording Surface	0-100
13 Depth of legroom in the knees	<400
14 Depth of space at foot level	<600
15 Knee space height	<600
16 Height of space at foot level	<100
17 Legroom width at level	<500
18 Footrest height	50-130

19 Footrest angle	0-25
20 Footrest Width	300
21 Footrest depth	400

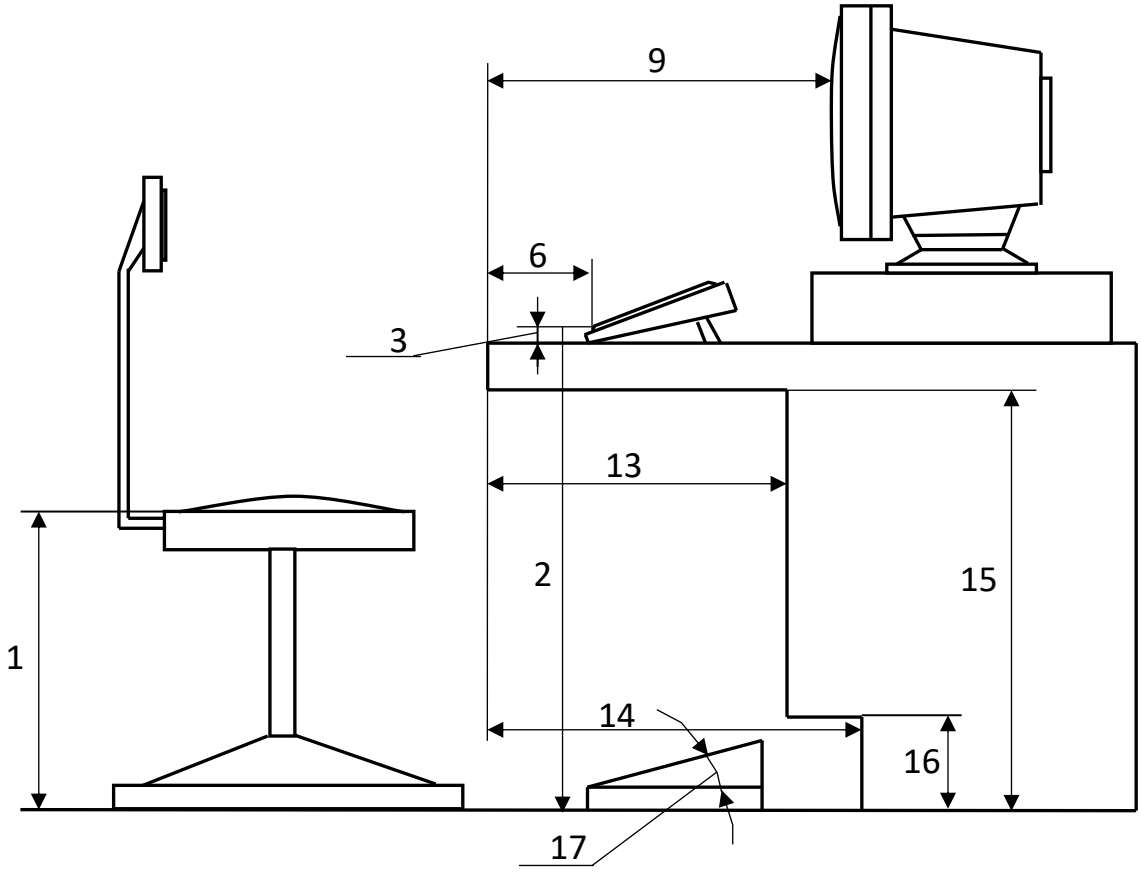

Fig. N Organization of the workplace

4.2.2 List of harmful and dangerous production factors

Currently, computer technology is widely used in all areas of activity, so it is very important to understand the dangerous and harmful factors to which a person is exposed during work:

а) electromagnetic fields (radio frequency range: HF, UHF and microwave)

б) infrared and ionizing radiation

в) static electricity

г) noise and vibration

д) poor lighting

4.2.3 Analysis of harmful and dangerous production factors

4.2.3.1 Influence of electromagnetic radiation

Permissible values of parameters of non-ionizing electromagnetic radiation from the computer monitor are presented in the table 4.2.[24]

Table 4.2 Permissible values of parameters of non-ionizing electromagnetic radiation

The name of the parameter	Allowable values
The intensity of the electric component of the electromagnetic field at a distance of 50 cm from the surface of the video monitor	10 V/m
The intensity of the magnetic component of the electromagnetic field at a distance of 50 cm from the surface of the video monitor	0,3 A/m
The electrostatic field strength should not exceed: for adult users for children of preschool institutions and students of secondary special and higher educational institutions	 20 kV/m 15 kV/m

The normalized parameter of unused X-rays is the exposure dose rate. At a distance of 5 cm from the surface of the monitor screen, its level should not exceed 10 μR / h. The maximum level of X-rays in the workplace of a diagnostic engineer usually does not exceed 20 μR / h. And the intensity of ultraviolet and infrared radiation from the monitor screen is in the range of 10 ... 100MW / m^2.

At a distance of 5-10 cm from the screen and the monitor body voltage levels can reach 140 V / m on the electrical component, which significantly exceeds the allowable values.

4.2.3.2 Exposure to noise and vibration

Noise worsens working conditions by having a harmful effect on the human body. Workers in conditions of prolonged noise experience irritability, headaches, dizziness, memory loss, fatigue, loss of appetite, ear pain, etc. Such disturbances in the work of a number of organs and systems of the human body can cause negative changes in the emotional state of man up to stress. Noise affects the digestive and circulatory system, the

cardiovascular system. In the case of a constant background noise up to 70 dB there is a violation of the endocrine and nervous systems, up to 90 dB - impairs hearing, up to 120 dB - leads to physical pain, which can be unbearable. Noise not only worsens human well-being, but also reduces labor productivity by 10-15%. In this regard, the fight against it is not only sanitary and hygienic, but also of great technical and economic importance [25].

In the table. 4.3 specified limit sound levels depending on the category of severity and intensity of work, which are safe to maintain health and efficiency.

The noise level in the workplace of diagnostic engineers engaged in calculations should not exceed 50dBA

Table 4.3 Limit sound levels, dB, in the workplace

Category labor intensity	Category of difficulty of work			
	I. Light	II. Medium	III. Heavy	IV.Very heavy
I. A little tense	80	80	75	75
II. Moderately tense	70	70	65	65
III. Strained	60	60	-	-
IV. Very strained	50	50	-	-

4.2.3.3 Influence of lighting

Properly designed and executed industrial lighting improves the conditions of visual work, reduces fatigue, increases productivity, has a beneficial effect on the production environment, providing a positive psychological effect on the worker, increases occupational safety and reduces injuries.

Insufficient lighting leads to eyestrain, weakens attention, leads to premature fatigue. Excessively bright lighting causes blindness, irritation and tearing in the eyes. The wrong direction of light in the workplace can create sharp shadows, glare, disorient the worker. All these causes can lead to accidents or occupational diseases, so it is important to correctly calculate the light.

4.3. Development of technical, organizational solutions that reduce the impact of harmful factors

This section will discuss technical and organizational solutions that ensure the health of workers as well as safe and harmless working conditions in the workplace of the diagnostic engineer.

4.3.1 Measures to reduce the impact of lighting

According to ДБН В.2.5-28-2006 in the premises of computer centers it is necessary to use a system of combined lighting

When performing work of the category of high visual accuracy (the smallest size of the object of distinction 0,3 ... 0,5 mm) the value of the coefficient of natural light (CNL) should be not less than 1,5%, and at visual work of average accuracy (the smallest size object of distinction 0,5 ... 1,0 mm) CNL should be not less than 1,0%. As sources of artificial lighting are usually used fluorescent lamps, which are combined in pairs into lamps, which should be located evenly above the work surfaces [26].

Requirements for lighting in rooms where computers are installed are as follows: when performing high-precision visual work, the total illumination should be 300 lux, and combined - 750 lux; similar requirements when performing work of medium accuracy - 200 and 300 lux, respectively

In addition, the entire field of view should be illuminated fairly evenly - this is a basic hygienic requirement. In other words, the degree of illumination of the room and the brightness of the computer screen should be approximately the same, because bright light in the area of peripheral vision significantly increases eye strain and, as a consequence, leads to their rapid fatigue.

The workplace should be placed in such a way as to avoid direct light in the eyes. To ensure protection and achieve standardized levels of computer radiation, it is necessary to use screen filters, local light filters (personal eye protection) and other means of protection that have been tested in accredited laboratories and have an annual hygienic certificate. [27]

Also, the current lighting of the room should be carried out by a system of general uniform lighting. In premises at predominant work with documents use of system of the combined lighting, ie installation of fixtures of local lighting in addition to the general is allowed [27].

4.3.2 Measures to reduce the effects of electromagnetic radiation

To reduce the effects of these types of radiation, it is recommended to use monitors with low radiation levels (MPR-II, TCO-92, TCO-99), install protective screens, as well as adhere to regulated modes of work and rest.

At the design stage of the room, the relative position of the irradiating objects must be ensured, which minimizes the influence of electromagnetic radiation.

4.3.3 Solutions to reduce the effects of noise and vibration

To reduce the noise level, the walls and ceiling of rooms where computers are installed can be lined with sound-absorbing materials. The level of vibration in the premises of the experiments can be reduced by installing equipment on special vibration isolators.

4.4 Fire Safety

Fire prevention should not be neglected, as the correct assessment of the fire hazard of the house, the identification of dangerous factors and justification of methods and means of fire prevention and protection.

If we look into the Правила пожежної безпеки в Україні НАПБ А.01.001-14.(чинний від 2014-12-30.) we can see that laboratories belong to category C, so our building must be equipped by 5 fire extinguishers of different types and fire alarm system, also it has to be buckets with sand.

The most important condition for fire safety is the elimination of possible sources of inflammation that may be:

a) faulty electrical equipment, faults in electrical wiring, electrical outlets and switches.

To exclude the occurrence of fire for these reasons, it is necessary to timely identify and eliminate faults, conduct a scheduled inspection and timely eliminate all faults.;

б) faulty electrical appliances.

Necessary measures to eliminate the fire include timely repair of electrical appliances, high-quality correction of breakdowns, non-use of faulty electrical appliances;

в) space heating with electric heating devices with open heating elements.

Open heating surfaces can cause a fire because there are paper documents and reference books in the form of books, manuals, and paper is a flammable material. In order to prevent fire, I suggest not to use open heaters in the laboratory;

г) short circuit in the wiring.

In order to reduce the likelihood of a fire due to a short circuit, it is necessary that the wiring was hidden;

е) non-compliance with fire safety measures and smoking in the room can also cause a fire.

To eliminate fires as a result of smoking in the laboratory, I propose to strictly prohibit smoking, and allow only in a strictly designated place.

To eliminate the possibility of fire, it is also necessary to conduct a periodic fire instruction, which will remind employees of fire safety rules.

4.5 Calculation of workplace lighting

The correct choice and calculation of the illumination of the workplace ensures the creation of normal conditions for the vision of the service personnel, and contributes to an increase in labor productivity. Sanitary lighting is the most important condition for occupational health and industrial culture. With good lighting, eye strain is eliminated, the pace of work is accelerated.

For rational lighting, the following conditions must be met:

– constant illumination of work surfaces;

– sufficient and evenly distributed brightness of illuminated work surfaces;

– lack of sharp contrasts between the brightness of the work surface and the surrounding space;

– the absence in the field of view of luminous surfaces with high brilliance, which is achieved by the use of lamps with diffused light and an increase in the height of their suspension.

For good lighting of rooms and workplaces, the choice of color for painting ceilings, walls and production equipment is of great importance..

Let's calculate the luminescent lighting of the office, designed to perform work with the size of the object of discrimination from 0.3 min to 1 min. The dimensions of the premises: A = 6 m, B = 3 m, H = 2.7 m. The area of the room is determined by the formula[28]:

$$S=A*B$$

Substituting the values, we get:

$$S=6*3=18 \text{ м2}$$

Lighting is designed using lamps with a minimum illumination of Emin = 200 lux, an average specific power of 17-23 W / m2. Suspension height above the working surface Hp = 1.7 m. Lighting is performed with LB-65 * 40 lamps, luminous flux of lamps Fl = 4550 lm, length 1.5 m, safety factor is equal to k = 1.5.

Determine the indicator of the room by the formula:

$$i=A*B/(Hp*(A+B))$$

Substituting the values, we get:

$$i=6*3/2*(6+3)=1$$

Then, for i = 1, the reflection coefficients of the ceiling Pp = 0.7 and the walls Pc = 0.5, we find the utilization factor of the luminous flux h = 0.41. The required number of lamps is determined by the formula [6]:

$$N=Emin*S*K*Z /Fл*h*n$$

where n = 2 is the total number of lamps in the luminaire.

Substituting the values, we get:

N=200*18*1,5/2480*0,37*0.9*2=3.3 lamps.

Assuming N=4;

The total number of lamps is n=2*4=8.

Thus, the fulfillment of the above requirements for the organization of the workplace will provide comfortable conditions for mental work.

5. Environment Protection

5.1 Introduction

Among all modes of transport, aviation occupies a special place. Due to its main advantage, namely saving time and convenience, people are increasingly choosing aviation as a form of movement between cities and countries, as well as continents. In today's world, aviation ranks 3rd in passenger traffic. Aviation also deals with the transportation of various cargoes, the timeliness of items that have the ability to deteriorate quickly, or if something needs to be transported urgently, although the main function of the aviation industry is to transport passengers. Due to this increase in the level of use of the aviation industry, it is necessary to understand its impact on the environment.

5.2 Pollution due to aviation

Modern turbojet engines use fuel to produce heat energy, which is then transferred from the turbine to the fan or blades. But the combustion of fuel, which consists mainly of hydrocarbons, as obtained by refining crude oil, emits carbon dioxide (CO_2), sulfur dioxide (SO_2) and steam (H_20). And so in addition to emissions from combustion, due to incomplete combustion of fuel, small particles of fuel, volatile organic compounds, carbon monoxide (CO) are added. We should not forget about the incomplete use of all the energy of gases, namely temperatures, high temperatures lead to the formation of oxides of nitrogen (NOx). The aviation engine also produces substances such as methane (CH4) and nitrous oxide (N20), but their amount is negligible, so their impact will not be considered.

The largest number of emissions into the environment per unit time occurs within airports during takeoffs and landings, during takeoffs the engine runs at maximum mode. But the largest amount of emissions into the atmosphere occurs in the troposphere, as most of the time he spends there, on cruising mode. Direct emissions into the troposphere have a greater impact than emissions on the earth's surface.

Direct analysis and measurement of the origin of air pollution is quite difficult, because the atmosphere and pollution with it, is constantly in motion and also changes chemically.

The increase in the use of aviation in passenger traffic from 1960 to 1990 increased by 9% each year, after growth fell to 2%, while scientific and technological progress is not standing still, and the development of more economical and environmentally friendly engines is also not standing still. As shown in Figure 5.1, the time of fuel consumption in modern engines is less than the samples of 60-70 years of the last century.

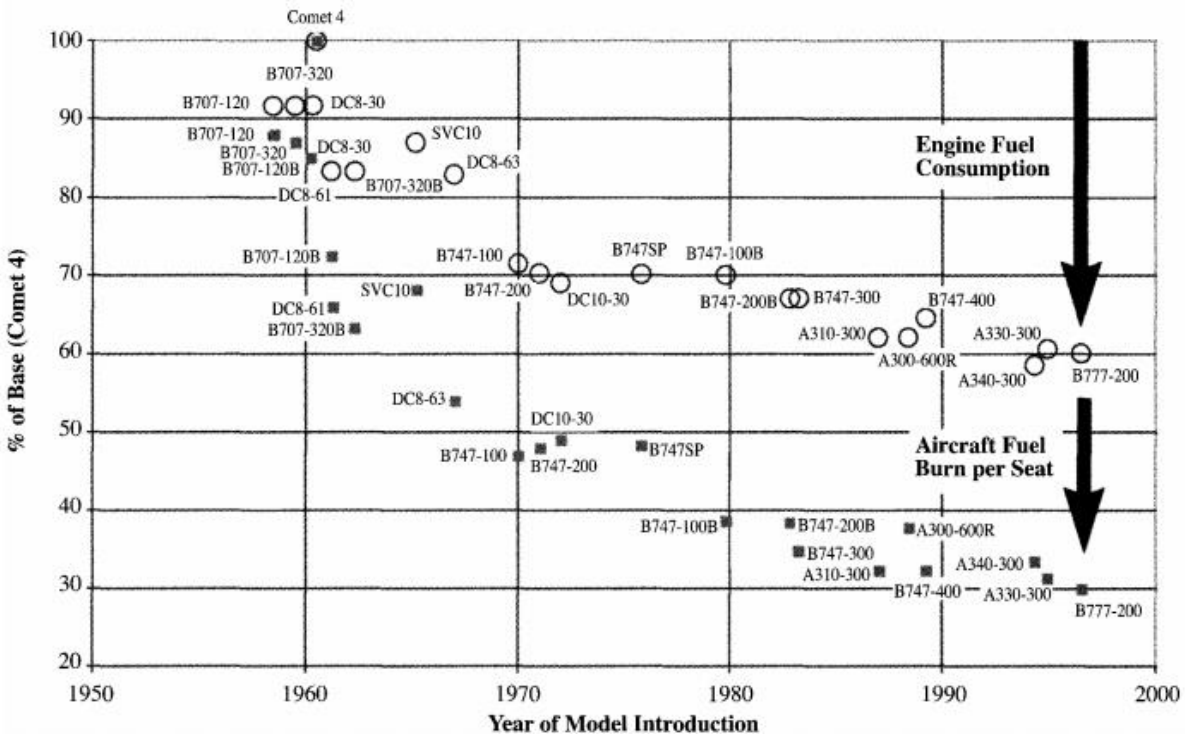

Fig. 5.1 Trend in transport aircraft fuel efficiency [30]

In [30], the growth of aviation emissions was forecast for 2015, and was 3 times higher than in 1990. The real picture of CO2 emissions for 1990, 2013, 2018, 2019 is presented in Table 5.1

Таблиця 5.1

Developments in world aviation emissions of CO2

Emissions	CO2

	Mton	Index (1990 = 1)
Emissions 1990	498	1.0
Emissions 2013	592	1.18
Emissions 2018	766	1.54
Emissions 2019	785	1.57

As we can see from Table 5.1, the steady growth of aviation has increased CO2 emissions by 57%.

Also in [31] the development and forecast of aviation emissions from 1990 to 2050, which is shown in Figure 5.2

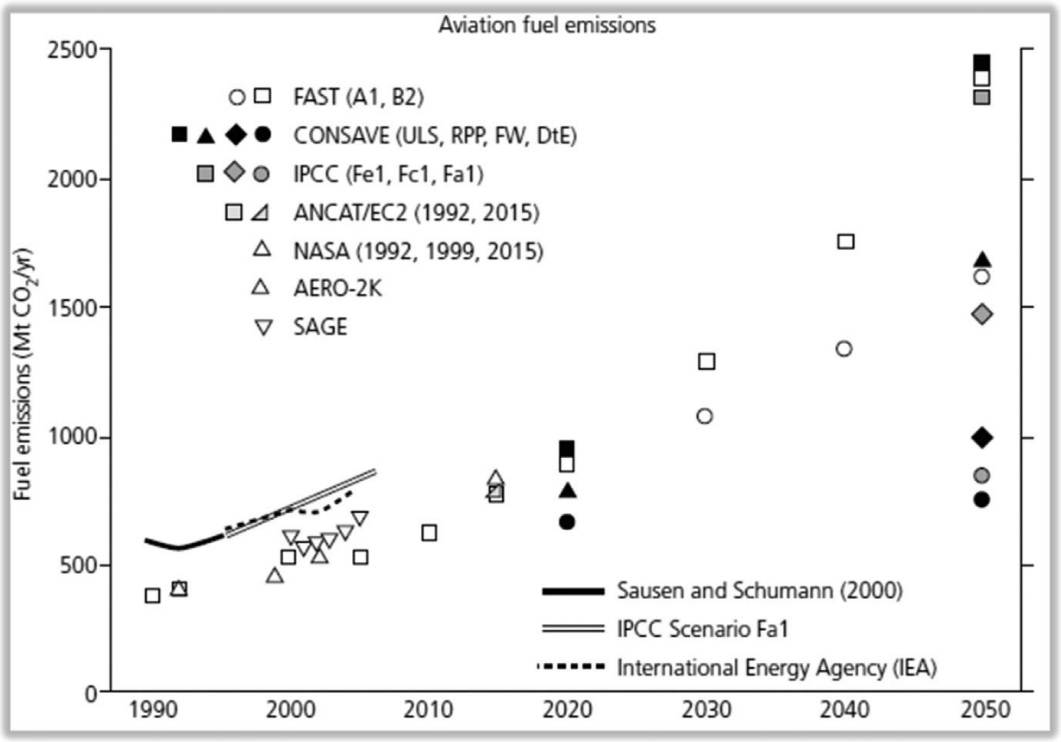

Fig 5.2 Fuel emissions of CO2 (metric tons per year) for 1990–2050.[4]

5.3 Noise pollution

Aviation noise - is part of the "sound background", it is heard every day by people from cities, towns and villages. Airports are close by and in the cities themselves, and aircraft routes pass through different parts of the country, even in the least populated areas

you can hear the plane flying somewhere. In cities where the environment is already exposed to heavy loads, aviation noise affects the quality of life, much more visible.

The problem with aircraft noise arose during the development of civil and military aviation, as the weight of the cargo to be transported increased the thrust of the engines, the size of the engines and the result was an increase in aircraft noise.

There are 3 types of noise pollution from aviation, namely:

- Mechanical noise
- Aerodynamic noise
- Noise from aircraft systems

Mechanical noise - is the noise from the fan blades, blades on the TPE, blades on the helicopter, as well as the speed of the engine. Most of the noise in aircraft with TPE create blades, as well as propellers. Turbofan engines, in turn, make the most noise at takeoff when the engine speed reaches its maximum. Also, the TPE at the output have a high-velocity gas jet, which is unstable and forms ring vortices, which in turn create noise. The sound level and the speed of the gases at the exit of the engine are proportionally related, so the minimum reduction in the speed of gas flows, reduces noise.

Aerodynamic noise - is the noise from aerodynamic flows, which are formed near the surfaces of the aircraft, such as the fuselage, wings and rudders and altitudes, usually when flying at low altitudes or high speeds. Aerodynamic noise increases when flying in a denser atmosphere or at increased speeds. Also, this type of noise is the main noise from the blades, due to the movement of air near the blades of either a turbofan engine or helicopter blades. Noise is also generated by the passage of a stream near parts of the aircraft, such as the landing gear.

Noise from aircraft systems - the main sources of noise are boost and air conditioning systems of the cabin and cabin. But the biggest sources of noise from aircraft systems are the APU, the onboard electric generator to run the APU.

Supersonic aviation also creates specific noise. When the plane of speed of sound crosses the air density jump, or as it is called this process shock wave, this thin transitional

area, where the transition of air into a denser area. The shock wave propagates in the opposite direction from the motion of the aircraft and forms a cone of density jump. When this wave reaches the earth, we can perceive it as a short-term sound shock.

With the increase in size, construction and mass increases the intensity of noise generation by this aircraft.

Many noise sources are present at airports, both in cities and beyond. Usually the acoustic environment in cities is not so favorable, in addition to aviation noise, which further affects the human body, as well as people living in the vicinity of airports, and airport staff and aircraft crew. At the same time, the number of people suffering from aviation noise is constantly growing, over time, due to the increase in the number of people living near the airport and the relentless development of aviation.

The level and amount of aircraft noise also depends on the direction of the runway and flight routes of aircraft, as shown in Figure 5.3, season and weather, as they depend on the intensity of flights

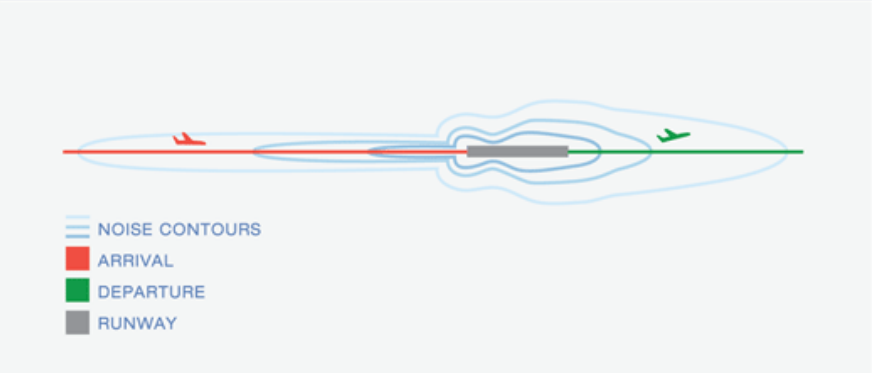

Fig. 5.3 Noise Contours

As we can see from the research in Los Angeles [32] the noise level of the airport near residential buildings ranges from 60 to 75 dB, due to its specific location on the ocean, it should be noted that in this case, of course, residential buildings are less affected due to takeoff, but we should not forget the coastal sea area this has an impact on the ecosystem of coastal residents.

5.4 Aviation and environmental impact

Aviation emissions affect air quality and also the global climate in the world. Compared to other emissions, aviation emits only 2% of all human pollution. But it still affects the environment, and pollution also occurs at high altitudes in the troposphere, which means that pollution covers a much larger area.

Although engines are becoming much more economical and environmentally friendly, but with the growth of flights, the total number of pollution is growing.

Berkeley G. Johnson, this chemist at the University of California in 1971 put forward a hypothesis that spoke about the impact of exhaust fumes from aviation on the environment.

Climate effects are due to interaction with solar and thermal radiation by gases such as carbon-dioxide and water vapor (see Figure 5.4 below), as well as pollutants such as CO, HC and black carbon (BC) particles arising from incomplete combustion in the gas turbine combustor[32]. SO_x emissions form sulfuric acid in the presence of water vapor, which further interacts with ammonia (NH_3) in the Earth's boundary layer to form ammonium sulfate particles[32]. NO_x emissions affect the formation of ozone and form nitric acid (HNO3) at cruise altitudes and ammonium nitrate particles in the boundary layer in the presence of ammonia, thus affecting air quality[32]. The soot particles at cruise altitudes interact with other chemicals such as sulfuric acid and nitric acid to form small particles that act as nucleating sites for condensation of water vapor present in the upper atmosphere under certain conditions to form larger particles to form condensation trails or contrails, for short[32]. These contrails are visible along flight tracks with a short lifetime around a few hours[32]. At times, under the right meteorological conditions these contrails expand perpendicular to the flight tracks to form contrail-induced cirrus clouds that also interact with shortwave and longwave radiation, thus affecting climate[32].

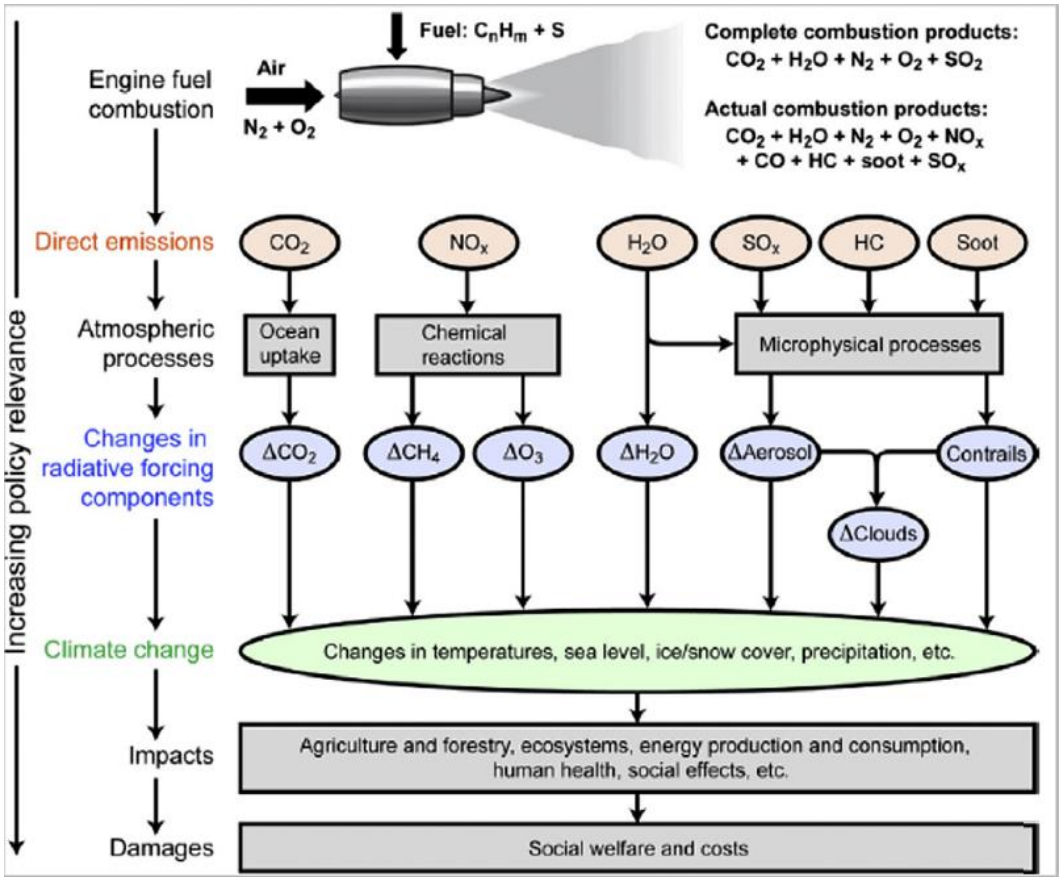

Fig. 5.4 Schematic showing emissions, processes, and possible impacts. HC, hydrocarbons[4]

Combustion of solid fuel combustion chamber emits H_2O, CO_2, HCl, CO, NO, Cl, as well as solid Al_2O_3 particles with an average size of 0.1 μm (sometimes up to 10 μm).

Airports, namely their surroundings, are affected by pollution, which causes groundwater pollution, mainly due to non-complete combustion of fuel and its leakage. Near airports, during takeoff, the engine emits liquid and gaseous contaminants, which after some time settle in the surrounding area.

The IPCC (2013) has provided estimates of the quantities of carbon in various earth systemcomponents. Fig. 5.5 presents a graphic of the data contained in the IPCC report (IPCC, 2013), showing the global carbon cycle including biological processes[31].

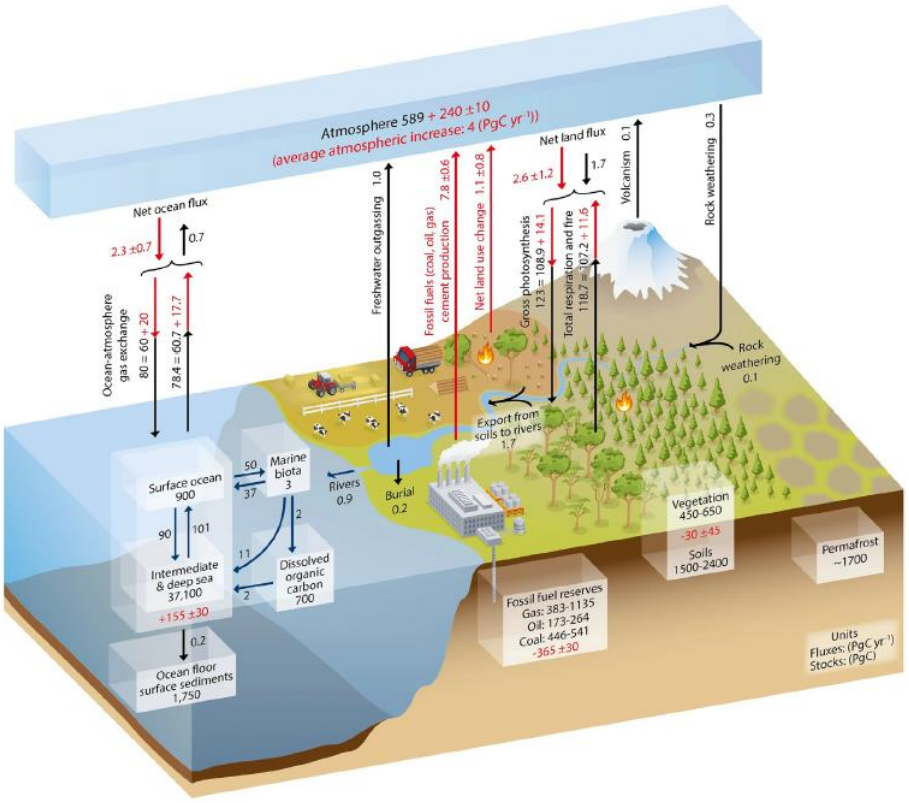

Fig. 5.5 Global carbon cycle[31].

Petroleum fuel particles, namely hydrocarbons, have the ability to penetrate to a depth, and quite large. For example, in porous rocks, aviation fuel penetrates more than 700 m in depth in 5 months. The best method is to prevent such penetration, to carry out preventive drilling of wells for water intake and subsequent testing. If there is a catastrophe and oil particles get into the water, it is pumped out and filtered through special filters.

Also on the surface of the runway accumulates a mixture of worn tires, pollen formed from fuel combustion, and other materials.

Noise, fairly quickly, causes the balance in ecosystems to be out of balance. A large amount of noise leads to poor orientation in space, causing difficulties in finding food and communication in animals. Because of this, some animals try to block this noise with louder screams, so it causes a chain reaction, and the animals themselves make more noise and further disrupt the ecosystem..

A striking example of this imbalance due to noise pollution can be, not isolated cases, the release of dolphins ashore, due to the use of sonar, which led to a loss of orientation in the space of animals. The same loss of orientation occurs in bees, due to the

noise of a flying plane, in addition to this noise can harm the larvae of bees and up to their death.

Noise can impair and disrupt mental health, it can also be dangerous to their health. The number of people suffering from insomnia and cardiovascular disease caused by noise is increasing every year. Researchers and clinicians have found in recent years that being in a noisy environment is often the cause of phobias and aggression. Because noise of a person gets tired and you can not get used to it. High intensity sounds are painful.

Up to 90 dB, up to so many people normally perceive sound when the noise from a turbojet aircraft is more than 100 dB, and from hypersonic over 160 dB. If a person is exposed to noise for more than 90 dB for a long time, it can cause hearing loss. Noise also has an effect on cardiovascular disease. If the noise level is above 145 dB, it causes hearing loss - damage to the eardrums, or rather their rupture.

5.5 How to solve the problems

To reduce the impact of pollution on the environment, you can reduce the number of particles emitted by the engine during combustion, namely the use of more economical air-fuel mixtures (mixing them in the combustion chamber). Development of better combustion chambers for better fuel spraying, and development of more reliable fuel systems.

Developing more economical engines will allow us to reduce the amount of fuel that will burn, which in turn will reduce the amount of pollution. Also at the moment there is a search for more environmentally friendly and "cleaner" fuels.

To reduce noise, designs are being developed that will reduce the amount of aerodynamic noise from the flow behind the engine, as well as reduce vibration from the engine.

5.6 Affect of my research

The assessment method I am working on in this paper will allow us to more accurately assess turbine blade damage, which will give us an understanding of when to

replace or repair blades so that the blades can better absorb thermal and kinetic energy from the flow. gases, which in turn will reduce emissions

REFERENCES

1. ДСТУ 2860–94 «Надійність техніки. Терміни та визначення», чинним від 01.01.1996 р

2. Н. Н. Смирнова Техническая експлуатация ЛА /под. ред. Н. Н. Смирнова. Москва «Транспорт» 1990г – 70с.

3. Игнатович, М.В. Карускевич, Т.П. Маслак, С. С. Юцкевич. Ресурс и долговечность авиационной техники: учеб. пособ. / С.Р.. – К. : НАУ, 2015. – 164 с.

4. А. И. Пугачева. Техническая эксплуатация летательных аппаратов. Под ред. А. И. Пугачева. Учебник для вузов гражданской авиации. Изд. 2-е, перераб. И доп. М., «Транспорт», 1977 – 440с.

5. AC 25.571-1C Damage Tolerance and Fatigue Evaluation of Structure. Department of Transportation. Federal Aviation Administration, 4/29/98.

6. Болотин В.В. Прогнозирование ресурса машин и конструкций. - М.: Машиностроение, 1984. - 312 с.

7. Акимов В. М. Основы надежности газотурбинных двягателей: Уч. Для студентов машиностроительных специальностей вузов. - М.; Машиностроение, 1981.- 207 с.

9. Березин И.Я., Чернявский О.Ф. Сопротивление материалов. Усталостное разрушение металлов и расчеты на прочность и долговечность при переменных напряжениях: Учебное пособие. Под общей редакцией О.Ф.Чернявского. – Челябинск: Изд. ЮУрГУ, 2003. – с.76

10. Болотин В.В. Ресурс машин и конструкции. – М.: Машиностроение, 1990. – 448 с

11. Терентьев В. Ф., Кораблева С.А. Усталость метталов.

12. Ашихмин В.Н., Гитман М. Б., Келлер И. Э. Введение в математическое моделирование: Учеб. Пособие/Под ред. П.В. Трусова – М.:Логос,2005 - 440с.

13. V.V Yakimenko L.G. Volyanska, V.V. Panin, I.I. Gvozdetsky Thermodynamic and gas-dynamic calculations of aircraft fas turbine engine: Methodical guide for writing the course paper. Kyiv: NAU, 2003 -104p.

14. С.А. Дмитриев, И.Г. Цыбалов, Н.И. Шпакович Расчет и построения полетных характеристик ГТД нражданской авиации: Методические указания по курсовому и дипломному проектированию – Киев: КИИГА, 1984 – 36с.

15. CFM International CFM56 – https://aeronautica.online/engines/cfm-international-cfm56/

16. F. R. Larson & J. Miller, Transactions ASME, Vol. 74, p. 765–771, 1952.

17. В.Ф. Березлев, И.И. Гвоздецкий, Е.Н. Карпов Констркция и прочность авиационніх газотурбинных двигателей: Методическое руководство по выполнению курсового проекта – Киев: КИИГА, 1977г

18. DOT/FAA/CT-89/7 Statistics on Aircraft Gas Turbine Engine Rotor Failures that Occurred in U. S. Commercial Aviation During 1985

19. Резинских. В.Ф. Исследование изломов. Методические рекомендации и атлас повреждений деталей проточной части турбин Москва -1993.

20. Термопрочность деталей машин. Под ред. И.А. Биргера и Б.Ф.Шорра. М., "Машиностроение", 1975. - 455с.

21. Yakushenko O. Influence of random factors on gas turbine engine constructive elements damage estimation / O. Yakushenko, P. Korolov, O. Popov, A. Mirzoev, V. Miltsov, O. Surovtsev//Матеріали XIV МНТК 23-25 квітня 2019 р. "Авіа–2019".–К.: НАУ, 2019. – С.20.1-20.6

22. Cyrus Meher-Homji, Andrew F. Bromley, Jean-Pierre Stalder gas turbine performance deterioration and compressor washing. Turbomachinery Laboratory, Texas A&M University 2013

23. Безпека життєдіяльності. / Под ред. Н.А. Бєлова - М.: Знання, 2000 - 364с.

24. Санітарні норми мікроклімату виробничих приміщень [Електронний ресурс] : ДСН 3.3.6.042-99. – Чинний від 1999-12-01. – К. : МОЗ України, 1999. – URL: http://zakon2.rada.gov.ua/rada/show/va042282-99. – (Державні санітарні норми)

25. Гігієна праці та експертиза умов праці [Електронний ресурс] : https://uz.dsp.gov.ua/index.php/diialnist/hihiiena-pratsi/749-shum-ta-ioho-shkidlyvi-naslidky

26. ОСНОВИ ОХОРОНИ ПРАЦІ ТА ОХОРОНА ПРАЦІ В ГАЛУЗІ Електронний навчальний посібник / Ю.Г.Масікевич, Т.І.Грачова, О.М.Жуковський, І.Д.Візнюк – Чернівці: БДМУ, 2015

27. Державні санітарні правила і норми роботи з візуальними дисплейними терміналами електронно-обчислювальних машин [Електронний ресурс] : ДСанПіН 3.3.2.007-98. – Чинний від 1998-12-10. – К. : МОЗ України, 1998. – URL: http://mozdocs.kiev.ua/view.php?id=2445. – (Державні санітарні правила та норми)

28. Природне і штучне освітлення. [Текст]: ДБН В.2.5-28-2018. – На заміну ДБН В.2.5-28-2006; чинний з 2019-03-01. – К. : Мінрегіон України, 2018. – 133 с. – (Державні будівельні норми України)

28. Fact Sheet | The Growth in Greenhouse Gas Emissions from Commercial Aviation (2019) / Jeff Overton Retrieved from https://www.eesi.org/papers/view/fact-sheet-the-growth-in-greenhouse-gas-emissions-from-commercial-aviation

29. NL Ministry of Housing, Spatial Planning and the Environment, Directorate for Noise and Traffic, P.O. Box 30945, 2500 GX The Hague, The Netherlands

30. Vedantham, A. (1999). Aviation and the Global Atmosphere: A Special Report of IPCC Working Groups I and III. Retrieved from https://repository.upenn.edu/library_papers/61

31. R. Alberto Bernabeo1, Evan K. Paleologos1, Abdel-Mohsen O. Mohamed Tropospheric air pollutiondaviation industry’s case // Abdel-Mohsen O. Mohamed, Evan K. Paleologos and Fares M. Howari Pollution Assessment for Sustainable Practices in Applied Sciences and Engineering | ScienceDirect, 2021 – 583-637 pp Retrieved from

https://www.sciencedirect.com/book/9780128095829/pollution-assessment-for-sustainable-practices-in-applied-sciences-and-engineering#book-info

32. Los Angeles International Airport 5-1 / 14 CFR Part 150 Noise Exposure Map Report 2015 Retrieved from: https://www.lawa.org/-/media/lawa-web/noise-management/files/150-noise-exposure/14cfrpart150_finalnemreport_lax-ch5.ashx